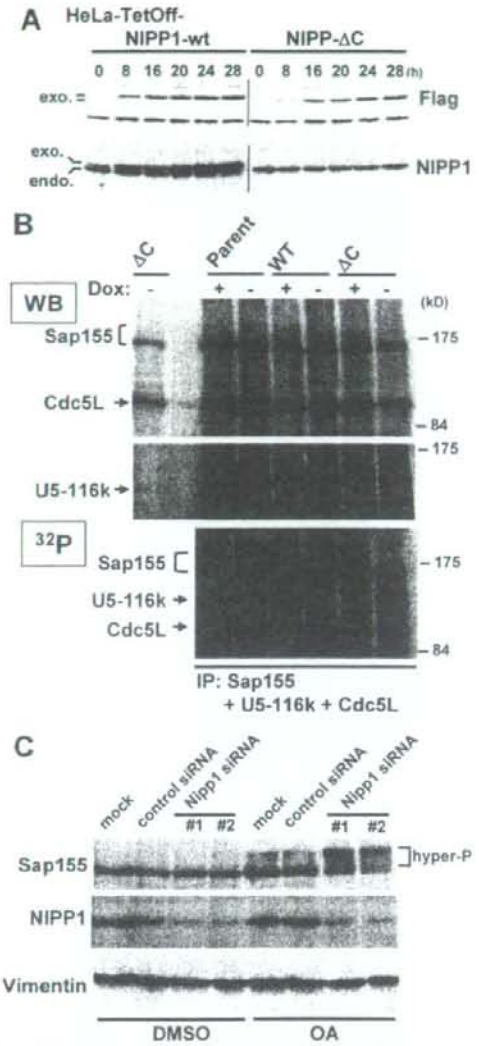

FIGURE 5. **Regulation of Sap155 phosphorylation by NIPP1 in intact cells.** *A*, establishment of HTO clones conditionally expressing exogenous NIPP1. HTO-NIPP1 clones maintained in 5 ng/ml Dox were washed and cultured in the absence of Dox for the times indicated. Cell lysates were subjected to immunoblotting with the anti-FLAG antibody (*upper*) or the anti-NIPP1 antibody, which recognizes the Lys-rich region of NIPP1 (*lower*). The positions of exogenous and endogenous NIPP1 are shown at the left as *exo.* and *endo.*, respectively. *B*, parental HTO and stable clones were cultured in the presence or absence of 10 ng/ml Dox. After 24 h, cells were labeled with ^{32}P-orthophosphate for 4 h. Sap155, U5-116k, and Cdc5L were simultaneously immunoprecipitated by the corresponding antibodies, fractionated by SDS-PAGE, and transferred to a nitrocellulose membrane. The membrane was first immunoblotted with the mixture of mouse monoclonal anti-Sap155 and anti-Cdc5L antibodies, and then with rabbit anti-sera against U5-116k (*WB*). Subsequently, the membrane was subjected to autoradiography (^{32}P). A portion of lysate was also loaded onto the gel to reveal positions of the three proteins shown at the *left*. *C*, HTO cells were transfected with control siRNA or siRNAs against human NIPP1. Forty eight hours later, transfected cells were incubated an additional 4.5 h with 100 nM okadaic acid (*OA*) or vehicle (DMSO). Immunoblots were performed using anti-Sap155, anti-NIPP1, or anti-vimentin antibodies.

with NIPP1-WT was highly phosphorylated. These results are consistent with previous reports that NIPP1/Sap155 interaction requires both the NIPP1 FHA domain and Sap155 phosphorylation (19). Furthermore, interaction between NIPP1 FHA and Sap155 appears to require that Sap155 be "hyper"-phosphorylated because a faster migrating Sap155 species seen on SDS-PAGE was likely phosphorylated at relatively low levels (autoradiography in Fig. 5*B*) and was not significantly co-immunoprecipitated with NIPP1-WT. Notably, NIPP1-RATA, which binds PP1 less efficiently than NIPP1-WT, co-immunoprecipitated hyperphosphorylated Sap155 more efficiently than did NIPP1-WT. In contrast, NIPP1-ΔC again decreased hyperphosphorylation of Sap155 based on its mobility shift ("lysate" in Fig. 7*A*), and hence did not co-immunoprecipitate Sap155 ("IP" in Fig. 7*A*). Collectively, these results indicate that PP1, which is recruited to hyperphosphorylated Sap155 by NIPP1 through the FHA domain, dephosphorylates Sap155 and suggest that its de-regulation by a mutant form of NIPP1, NIPP1-ΔC, results in defects in pre-mRNA splicing. Strikingly, the NIPP1 mutants NIPP1-RATA/ΔC and -R53A/ΔC, which harbor second mutations that no longer inhibit splicing (Fig. 3), also failed to reduce levels of Sap155 hyperphosphorylation (Fig. 7*B*).

PP1 Overexpression Compromises Pre-mRNA Splicing—Three PP1 isoforms exhibiting differing N- and C-terminal sequences (PP1α, PP1γ1, and PP1δ) are expressed in mammalian somatic cells. To determine which isoforms bound to NIPP1, co-immunoprecipitation experiments were performed. Significant amounts of PP1α, the most abundant isoform expressed in HeLa cells, but not PP1γ1 and PP1δ, co-immunoprecipitated with endogenous NIPP1, in the order PP1α ≫ PP1γ1 > PP1δ (Fig. 8*A*). Because NIPP1 recruited PP1 to dephosphorylate Sap155 and NIPP1 dysregulation resulted in splicing inhibition, one might predict that excess nuclear PP1 might also inhibit splicing. To test this possibility, the effects of PP1 overexpression on Sap155 phosphorylation and splicing were investigated. Hyperphosphorylated forms of Sap155 were reduced in cells transfected with PP1α-WT and PP1α-T320A but not in cells transfected with the inactive PP1α mutant, PP1α-H125A (Fig. 8, *C* and *D*). As expected, either overexpression of wild-type or the active mutant of PP1α, PP1c-T320A, compromised splicing of the reporter gene (Fig. 8*E*). In contrast, the inactive PP1α mutant, PP1α-H125A had no effect.

DISCUSSION

In this study, we investigated physical and functional association between NIPP1, PP1, and pre-mRNA splicing *in vivo*. Recently, it was reported that PP1 and/or PP2A are required for a catalytic step in splicing, specifically the second step, *in vitro* and that Sap155 and U5-116k are potential targets of these two PPases (6). But how these PPases are recruited to spliceosomal substrates has not been elucidated. Our results demonstrate that NIPP1 targets PP1 to Sap155. Because NIPP1 has been considered a PP1 inhibitor, the stimulating effect of NIPP1 on Sap155 dephosphorylation by PP1 is unanticipated. These observations are reminiscent of Mypt1, another PP1 regulatory protein. Mypt1 inhibits PP1 activity against nonphysiological substrates such as phosphorylase *a* but stimulates it against

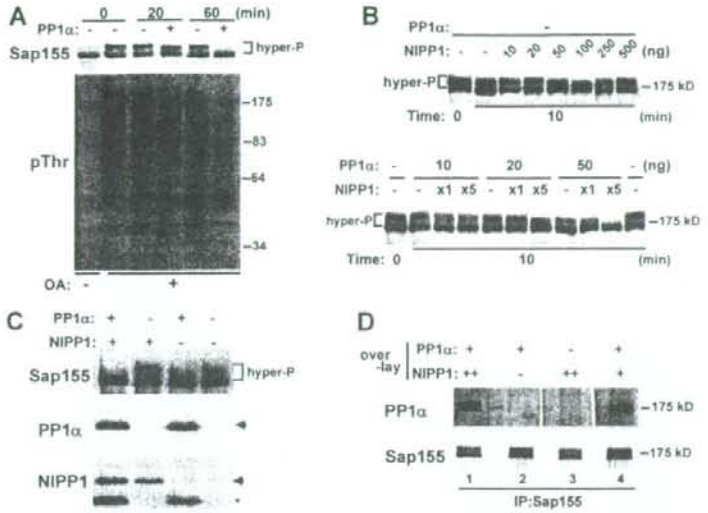

FIGURE 6. **NIPP1 bridges Sap155 and PP1.** *A*, dephosphorylation of Sap155 by PP1 *in vitro*. HTO cells were transfected with siRNA against NIPP1, treated with OA, and lysed. Lysates were incubated with 50 ng of recombinant PP1α at 30 °C for the times indicated. Immunoblots were done with anti-Sap155 or anti-*pThr* antibody. *B*, NIPP1 enhances Sap155 dephosphorylation by PP1 *in vitro*. Lysates of OA-treated HTO cells were incubated with increasing amounts of exogenous NIPP1 (*upper*) or PP1-NIPP1 holoenzyme (*lower*) at 30 °C for 10 min. Immunoblots were done with anti-Sap155 antibody. The holoenzyme was reconstituted using recombinant PP1α and His-NIPP1 expressed in and purified from *E. coli*. *Lower panel*, NIPP1 amounts are shown as a ratio relative to recombinant PP1α. *C*, dephosphorylation experiments using purified Sap155. *In vitro* dephosphorylation experiments were performed, as in *B*, using Sap155 immunopurified from HeLa cells treated with OA. Reactions were done using 50 ng of PP1α and/or His-NIPP1 per reaction and analyzed by immunoblot using anti-Sap155, anti-PP1α, and anti-NIPP1 antibodies. *Asterisk* marks residual signal of anti-PP1α blot. *D*, reconstitution of Sap155-NIPP1-PP1 ternary complex *in vitro*. Physical association between Sap155 and PP1 was analyzed by far-Western. Sap155 was immunoprecipitated, size-fractionated by SDS-PAGE, and transferred to a membrane. Membrane pieces were reacted with 100 ng/ml of PP1α in the presence or absence of recombinant His-NIPP1 (++ and + indicate 300 and 100 ng/ml His-NIPP1, respectively). PP1α overlaid on Sap155 was detected by immunoblot using anti-PP1α antibody. Similar amounts of Sap155 in each lane were confirmed by anti-Sap155 blot (*lower*).

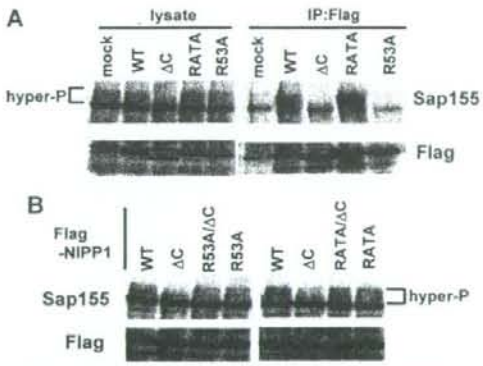

FIGURE 7. **Physical and functional associations between NIPP1 mutant proteins and Sap155.** *A*, ΔC mutation of NIPP1 decreases Sap155 phosphorylation and results in dissociation of the NIPP1-Sap155 complex. HTO cells were transfected with FLAG-NIPP1 plasmids. Twenty eight hours later, cells were lysed and subjected to immunoprecipitation (*IP*) with an anti-FLAG antibody. Immunoprecipitates were analyzed by immunoblot using anti-Sap155 or anti-FLAG antibodies. *Hyper-P* indicates positions of hyperphosphorylated forms of Sap155. *B*, reduction of hyperphosphorylated Sap155 by NIPP1-ΔC requires both a functional FHA domain and interaction with PP1. Cells were transiently transfected with FLAG-NIPP1 plasmids depicted in Fig. 1*A* and Fig. 3*A*, lysed, and immunoblotted with anti-Sap155 and anti-FLAG antibodies.

myosin light chain, a physiological substrate of the Mypt1/PP1 holoenzyme (35). We propose that the inhibitory activity of NIPP1 is also substrate-dependent.

Whereas overexpression of NIPP1-WT slightly reduced levels of hyperphosphorylated Sap155, expression of NIPP1-ΔC, which constitutes a hyper-active PP1 holoenzyme, produced more severe phenotypes, such as virtual loss of Sap155 hyperphosphorylation and defects in pre-mRNA splicing. The robust effect of NIPP1-ΔC is, at least in part, because of defects in regulation of the NIPP1-PP1 holoenzyme by inhibitory phosphorylation of the catalytic subunit. In contrast, PP1 bound to NIPP1-WT is highly phosphorylated at Thr-320. Although Thr-320 phosphorylation is implicated in regulating the cell cycle, our results suggest that regulation of PP1 by inhibitory phosphorylation is important in more general cellular functions, including regulation of pre-mRNA splicing. Recently, it was reported that Sf3a/b proteins, including Sap155, are destabilized and dissociate from the RNP core of the activated spliceosome during the transition from the B to C complex *in vitro* (5). Thus, it is likely that Sf3a and Sf3b are dispensable for the second splicing step while essential in early step(s). Given that PP1/PP2A are required for the second step, dephosphorylation of Sap155 may be critical for dissociation of Sf3a/b from the RNP core, facilitating structural rearrangement of the spliceosome required for further splicing steps. In this scenario, one could imagine that such regulation occurs by modulation of PPase activity through inhibitory phosphorylation of PP1 bound to NIPP1. Currently, why PP1 bound to NIPP1-ΔC is minimally phosphorylated on Thr-320 is not known and is under investigation.

Although our results show that NIPP1 enhances recruitment of PP1 to Sap155 and promotes Sap155 dephosphorylation, detailed mechanisms whereby NIPP1 stimulates Sap155 dephosphorylation remain unknown. It is important to determine how the PP1/NIPP1 holoenzyme can effectively and specifically dephosphorylate Sap155. PP1/NIPP1 interactions may be competed and transiently interrupted by element(s) within Sap155. Interestingly, Sap155 contains an RICF sequence (Arg-1057 to Phe-1060) resembling a consensus PP1-binding motif, although it has not been shown to be functional. Alternatively, NIPP1 may block substrates other than Sap155 from accessing the PP1 active pocket via steric hindrance. Future structural analysis of the PP1/NIPP1 holoenzyme should address these issues. In context, it is still possible that NIPP1 simultaneously

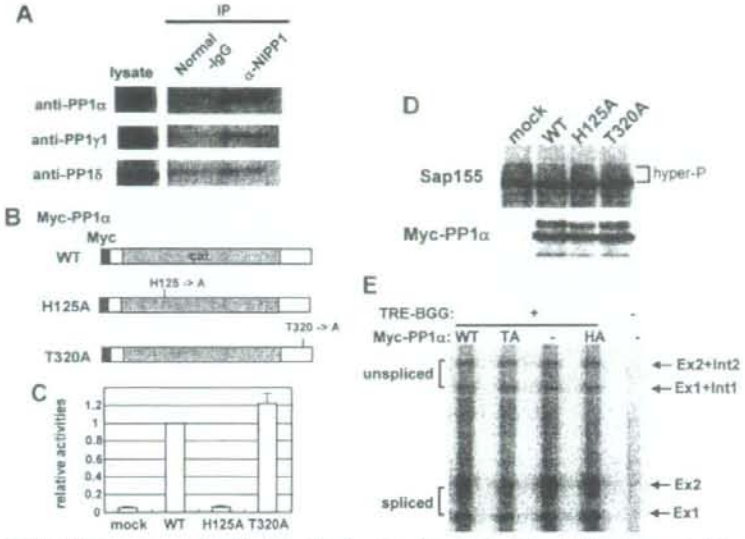

FIGURE 8. **PP1 overexpression affects Sap155 phosphorylation and splicing.** *A*, PP1 isoforms associating with NIPP1. Lysates of HTO cells were incubated with anti-NIPP1 antibody or control normal rabbit IgG. Immunoprecipitates (*IP*) were immunoblotted using antibodies specific to each PP1 isoform. *B*, diagram of wild-type and mutant forms of PP1α. Each is tagged with a Myc epitope at the N terminus. *C*, phosphatase activities of PP1α proteins expressed in HTO cells. Myc-PP1α were transiently expressed in HTO cells and immunoprecipitated with an anti-Myc antibody. Phosphatase activities were determined using phospho-phosphorylase peptide as substrate. Data represent means of three independent experiments with S.D. *D*, effects of PP1α overexpression on Sap155 phosphorylation. HTO cells were transiently transfected with myc-PP1α, lysed, and analyzed by Western blotting using anti-Sap155 and anti-Myc antibodies. *E*, cells were transiently transfected with the β-globin reporter together with myc-PP1α constructs. Total RNA was isolated and analyzed by RPA as in Fig. 2.

suppresses PP1 activity in a way that balances Sap155 phosphorylation activity to ensure proper phosphorylation/dephosphorylation cycle. Our results also do not exclude the possibility that higher activity of PP1-NIPP1ΔC against Sap155 *in vivo* is because of less inhibitory activity of the mutant NIPP1 itself. Currently, we cannot determine whether NIPP1-WT and -ΔC have similar inhibitory activity on hyperphosphorylated Sap155.

In cells expressing NIPP1-WT and -ΔC, Sap155 phosphorylation levels were specifically reduced, although normal phosphorylation levels of U5-116k were seen, suggesting de-regulation of Sap155 phosphorylation alone is sufficient to perturb splicing. But these results do not exclude the possibility that phosphorylation/dephosphorylation of U5-116k is also essential for splicing. Sap155 is the first example of a protein that phosphorylated exclusively at the time of the catalytic step of the splicing reaction (4). Indirect evidence has indicated the importance of Sap155 phosphorylation in splicing, although there has not yet been a direct demonstration. Our results provide additional evidence suggesting an essential role of Sap155 phosphorylation, namely NIPP1-ΔC constituted a hyper-active PP1 holoenzyme, decreasing hyperphosphorylated Sap155 and thereby inhibiting splicing. Sap155 has many potential phosphorylation sites, and several are phosphorylated in *in vitro* splicing reactions and also *in vivo* (36, 37). Identification of Sap155 phosphorylation sites and their functions during splicing is critically important for understanding how Sap155 is regulated byphosphorylation/dephosphorylation. Furthermore, recent reports revealed that Sap155 functions not only in constitutive splicing but also in alternative splicing and in epigenetic gene silencing (26, 38). Roles for Sap155 phosphorylation in these processes are the next questions to be analyzed.

NIPP1 knockdown sensitized Sap155 to hyperphosphorylation upon further stimulation of cells by OA. Because OA preferentially inhibits PP2A family PPases, our results are consistent with a previous report that PP1 and/or PP2A is essential for splicing *in vitro* (6). It is likely that PP1 and PP2A family PPase(s) indeed have overlapping roles in regulating Sap155 phosphorylation in intact cells. According to this notion, the relatively weak effects of mutant NIPP1 lacking the canonical PP1-binding motif (NIPP1-RATA) on splicing seem plausible. NIPP1-RATA was less efficient in binding PP1 and hence co-immunoprecipitated greater levels of hyperphosphorylated Sap155 compared with NIPP1-WT (Fig. 7), indicating that it functions as a dominant negative in some contexts, although its inhibition of splicing was partial (Figs. 1 and 2). One explanation for this observation would be that NIPP1-associated PP1 plays a kinetic role in splicing, affecting only splicing rate. Alternatively, we propose that lower levels of PP1 recruited by NIPP1-RATA could be compensated, for example, by PP2A class PPase(s). The relatively small increase in hyperphosphorylated Sap155 seen in mock- or control siRNA-transfected cells treated with OA (Fig. 5*C*) strengthens this hypothesis, although the precise mechanism by which OA enhances Sap155 hyperphosphorylation is not clear. As seen in Fig. 5*D*, treating cells with OA globally affected phosphorylation levels of several cellular proteins, possibly because of a broad spectrum of targets of PP2A class PPases or to indirect effects. Thus, we cannot exclude the possibility that OA enhances Sap155 hyperphosphorylation by stimulating Sap155 kinase(s). We tried co-transfection of siRNAs targeting PP2A in addition to NIPP, but massive cell death resulting from that treatment prevented analysis of these cells.[5] It is still possible that PP1 and PP2A dephosphorylate Sap155 differentially in terms of target residue or timing during splicing. Furthermore, PP1 and PP2A may be regulated differentially by intra- or extracellular signals through modification of the phosphatases themselves and/or

[5] N. Tanuma and M. Nomura, unpublished observations.

their regulatory protein. In addition to inhibitory phosphorylation of PP1, it should be noted that NIPP1 is also subject to regulation by phosphorylation, decreasing its association with PP1 (39, 40).

Interestingly, NIPP1-ΔC promoted severe splicing defects *in vivo* but not *in vitro*. Although *in vitro* splicing assays are reliable and widely used, they may not always reflect *in vivo* conditions, at least in terms of PP1. In fact, some investigators have reported differences between *in vivo* and *in vitro* splicing. For example, a sub-domain of U2AF65, an essential splicing factor, plays important role *in vivo* but not *in vitro* (41).

In summary, our results provide evidence that NIPP1 directs PP1 to dephosphorylate Sap155. Further elucidation of the role of the NIPP1 C terminus in regulating PP1 and identification of specific Sap155 sites dephosphorylated by PP1 will be required to fully understand how pre-mRNA splicing is regulated by protein phosphorylation/dephosphorylation cycles. Also, cell lines conditionally expressing NIPP1-ΔC, which mediates a decrease in Sap155 hyperphosphorylation, will be useful to analyze the roles of Sap155 phosphorylation.

Acknowledgments—We acknowledge Dr. H. Brahms and Dr. R. Lührmann (Max-Planck Institute, Göttingen, Germany) for kindly providing the anti-U5-116k antibody, and Dr. S. Ohno (Yokohama City University, Japan) for the pTRE-BGG plasmid (referred to as pTRE-β-globin in this paper). We also thank E. Yoshida for secretarial assistance.

REFERENCES

1. Misteli, T. (1999) *Curr. Biol.* **9,** R198–R200
2. Hastings, M. L., and Krainer, A. R. (2001) *Curr. Opin. Cell Biol.* **13,** 302–309
3. Stamm, S. (2008) *J. Biol. Chem.* **283,** 1223–1227
4. Wang, C., Chua, K., Seghezzi, W., Lees, E., Gozani, O., and Reed, R. (1998) *Genes Dev.* **12,** 1409–1414
5. Bessonov, S., Anokhina, M., Will, C. L., Urlaub, H., and Lührmann, R. (2008) *Nature* **452,** 746–750
6. Shi, Y., Reddy, B., and Manley, J. L. (2006) *Mol. Cell* **23,** 819–829
7. Ceulemans, H., and Bollen, M. (2004) *Physiol. Rev.* **84,** 1–39
8. Eto, M., Senba, S., Morita, F., and Yazawa, M. (1997) *FEBS Lett.* **410,** 356–360
9. Greengard, P. (2001) *Science* **294,** 1024–1030
10. Weiser, D. C., Sikes, S., Li, S., and Shenolikar, S. (2004) *J. Biol. Chem.* **279,** 48904–48914
11. Dohadwala, M., da Cruz e Silva, E. F., Hall, F. L., Williams, R. T., Carbonaro-Hall, D. A., Nairn, A. C., Greengard, P., and Berndt, N. (1994) *Proc. Natl. Acad. Sci. U. S. A.* **91,** 6408–6412
12. Yamano, H., Ishii, K., and Yanagida, M. (1994) *EMBO J.* **13,** 5310–5318
13. Berndt, N., Dohadwala, M., and Liu, C. W. (1997) *Curr. Biol.* **7,** 375–386
14. Liu, C. W., Wang, R. H., Dohadwala, M., Schönthal, A. H., Villa-Moruzzi, E., and Berndt, N. (1999) *J. Biol. Chem.* **274,** 29470–29475
15. Van Eynde, A., Nuytten, M., Dewerchin, M., Schoonjans, L., Keppens, S., Beullens, M., Moons, L., Carmeliet, P., Stalmans, W., and Bollen, M. (2004) *Mol. Cell. Biol.* **24,** 5863–5874
16. Egloff, M. P. F., Johnson, D., Moorhead, G., Cohen, P. T., Cohen, P., and Barford, D. (1997) *EMBO J.* **16,** 1876–1887
17. Beullens, M., Vulsteke, V., Van Eynde, A., Jagiello, I., Stalmans, W., and Bollen, M. (2000) *Biochem. J.* **352,** 651–658
18. Boudrez, A., Beullens, M., Groenen, P., Van Eynde, A., Vulsteke, V., Jagiello, I., Murray, M., Krainer, A. R., Stalmans, W., and Bollen, M. (2000) *J. Biol. Chem.* **275,** 25411–25417
19. Boudrez, A., Beullens, M., Waelkens, E., Stalmans, W., and Bollen, M. (2002) *J. Biol. Chem.* **277,** 31834–31841
20. Vulsteke, V., Beullens, M., Boudrez, A., Keppens, S., Van Eynde, A., Rider, M. H., Stalmans, W., and Bollen, M. (2004) *J. Biol. Chem.* **279,** 8642–8647
21. Durocher, D., Taylor, I. A., Sarbassova, D., Haire, L. F., Westcott, S. L., Jackson, S. P., Smerdon, S. J., and Yaffe, M. B. (2000) *Mol. Cell* **6,** 1169–1182
22. Kumeta, H., Ogura, K., Adachi, S., Fujioka, Y., Tanuma, N., Kikuchi, K., and Inagaki, F. (2008) *J. Biomol. NMR* **40,** 219–224
23. Beullens, M., and Bollen, M. (2002) *J. Biol. Chem.* **277,** 19855–19860
24. Trinkle-Mulcahy, L., Ajuh, P., Prescott, A., Claverie-Martin, F., Cohen, S., Lamond, A. I., and Cohen, P. (1999) *J. Cell Sci.* **112,** 157–168
25. Achsel, T., Ahrens, K., Brahms, H., Teigelkamp, S., and Lührmann, R. (1998) *Mol. Cell. Biol.* **18,** 6756–6766
26. Isono, K., Mizutani-Koseki, Y., Komori, T., Schmidt-Zachmann, M. S., and Koseki, H. (2005) *Genes Dev.* **19,** 536–541
27. Takizawa, N., Mizuno, Y., Ito, Y., and Kikuchi, K. (1994) *J. Biochem. (Tokyo)* **116,** 411–415
28. Yamashita, A., Ohnishi, T., Kashima, I., Taya, Y., and Ohno, S. (2001) *Genes Dev.* **15,** 2215–2228
29. Kim, S. E., Ishita, A., Shima, H., Nakamura, K., Yamada, Y., Ogawa, K., and Kikuchi, K. (2000) *Int. J. Oncol.* **16,** 751–755
30. Mitsuhashi, S., Shima, H., Tanuma, N., Matsuura, N., Takekawa, M., Urano, T., Kataoka, T., Ubukata, M., and Kikuchi, K. (2003) *J. Biol. Chem.* **278,** 82–88
31. Niranjanakumari, S., Lasda, E., Brazas, R., and Garcia-Blanco, M. A. (2002) *Methods (San Diego)* **26,** 182–190
32. Maniatis, T., and Reed, R. (2002) *Nature* **416,** 499–506
33. Friend, K., Lovejoy, A. F., and Steitz, J. A. (2007) *Mol. Cell* **28,** 240–252
34. Tran, H. T., Ulke, A., Morrice, N., Johannes, C. J., and Moorhead, G. B. (2004) *Mol. Cell. Proteomics* **3,** 257–265
35. Johnson, D., Cohen, P., Chen, M. X., Chen, Y. H., and Cohen, P. T. W. (1997) *Eur. J. Biochem.* **244,** 931–939
36. Seghezzi, W., Chua, K., Shanahan, F., Gozani, O., Reed, R., and Lees, E. (1998) *Mol. Cell. Biol.* **18,** 4526–4536
37. de Graaf, K., Czajkowska, H., Rottmann, S., Packman, L. C., Lilischkis, R., Luscher, B., and Becker, W. (2006) *BMC Biochem.* **7,** 7
38. Massiello, A., Roesser, J. R., and Chalfant, C. E. (2006) *FASEB J.* **20,** 1680–1682
39. Beullens, M., Van Eynde, A., Bollen, M., and Stalmans, W. (1993) *J. Biol. Chem.* **268,** 13172–13177
40. Van Eynde, A., Beullens, M., Stalmans, W., and Bollen, M. (1994) *Biochem. J.* **297,** 447–449
41. Banerjee, H., Rahn, A., Gawande, B., Guth, S., Valcarcel, J., and Singh, R. (2004) *RNA (N. Y.)* **10,** 240–253

Lung Cancer 63 (2009) 291–294

Contents lists available at ScienceDirect

Lung Cancer

journal homepage: www.elsevier.com/locate/lungcan

Four years experience of the survey on quality control of lung cancer screening system in Japan

Motoyasu Sagawa[a,*], Chiaki Endo[b], Masami Sato[c], Yasuki Saito[d], Tomotaka Sobue[e], Katsuo Usuda[a], Hirokazu Aikawa[a], Shigefumi Fujimura[b], Tsutomu Sakuma[a]

[a] Department of Thoracic Surgery, Kanazawa Medical University, 1-1 Daigaku, Uchinada, Ishikawa, Japan
[b] Department of Thoracic Surgery, Institute of Development, Aging and Cancer, Tohoku University, Sendai, Japan
[c] Department of Thoracic Surgery, Miyagi Prefectural Cancer Center, Natori, Japan
[d] Department of Thoracic Surgery, Sendai National Hospital, Sendai, Japan
[e] Center for Cancer Control and Information Services, National Cancer Center, Tokyo, Japan

ARTICLE INFO

Article history:
Received 22 December 2007
Received in revised form 24 April 2008
Accepted 13 May 2008

Keywords:
Screening
Cancer screening
Lung cancer
Quality control
Quality assurance
Survey

ABSTRACT

Although quality control is essential in mass screening system for early detection of cancer, no global method for quality control has not been established, because the mass screening system in each country is quite different from each other. At present, we have to find appropriate method for each cancer and for each country. In 2000, The Lung Cancer Screening Division (LCSD) of the Miyagi Prefectural Committee for Management of the Cancer Screening System (Miyagi PCMCSS) decided to evaluate annually whether the local governments had appropriate information to evaluate the quality of lung cancer screening systems, announcing that the results would be informed to residents. On the basis of the manual developed by the Ministry of Health, Labor and Welfare, 45 items were selected as indicators for the survey, which could be obtained easily when the screening had been conducted according to the standard method. LCSD of Miyagi PCMCSS sent a questionnaire including the 45 items to the municipalities. According to the reply to the questionnaire, LCSD rated each municipality using a 5-rank classification depend on the number of insufficient items: A: 0; B: 1–4; C: 5–8; D: 9 or more; E: no reply. As the results, 58, 3, 6, 3, and 0 municipalities were categorized in 2002 as A, B, C, D, and E, respectively. In 2003, the number of municipalities changed to 60, 7, 2, 1, and 0. In 2005, the distribution improved more, such as 68, 2, 0, 0, and 0. The detection rate of lung cancer also improved. It is possible for PCMCSS to annually conduct surveys to determine whether the local government has appropriate information to evaluate the quality of lung cancer screening systems. Such surveys improve the distribution of response to better direction.

1. Introduction

In mass screening system for early detection of cancer, quality control is essential. However, no global method for quality control which can be adopted in all countries has not been established, because the mass screening system in each country is quite different from each other. Although there have been some reports concerning quality control of mammography in breast cancer screening [1–3] and cytological diagnosis in cervical cancer screening [4,5], there has been few report about other examinations or other cancers [6,7]. At present, we have to find appropriate method for each cancer and for each country.

In Japan, mass screening for tuberculosis using chest X-ray films had been widely developed since 1950s. In 1982, lung cancer screening, using chest X-ray films for all screenees and sputum cytology for smokers, was introduced under the Health and Medical Services Law for the Aged [8,9]. According to the law, each local municipality conducts lung cancer screening for residents of 40 years old or older. For the quality control of the screening system, The Prefectural Committee for Management of the Cancer Screening System (PCMCSS) was established in each prefecture. Although the committee was expected to conduct appropriate quality control of the cancer screening, the activity of the committee in almost all of the prefectures has been very low. Most of them counted the number of screenees, test-positive rate, and lung cancer detection rate which were submitted from each municipality, but the quality of the data was not tested and no guidance or intervention was conducted to each municipality. The quality control of the screening system totally depended on the individual efforts of those who are

* Corresponding author. Tel.: +81 76 286 2211; fax: +81 76 286 1207.
E-mail address: sagawam@kanazawa-med.ac.jp (M. Sagawa).

0169-5002/$ – see front matter © 2008 Elsevier Ireland Ltd. All rights reserved.
doi:10.1016/j.lungcan.2008.05.012

in charge of screening activities in the municipality or the screening providers which was commissioned lung cancer screening from the municipalities. As a result, quality of the screening system has been quite different according to the municipality. Although PCMCSS does not have enough budget or personnel, some members of the committee thought that additional action should be taken.

In Miyagi Prefecture, Japan, the condition was almost the same as other prefectures until 2000. Some municipalities did not submit the data to PCMCSS, even after several demands to submit. In 2000, The Lung Cancer Screening Division (LCSD) of Miyagi PCMCSS decided to conduct a new survey for the quality control, which began in 2001. We present herein the 4-year results of the survey from 2001 to 2005.

2. Methods

In February 2000, LCSD of Miyagi PCMCSS decided to start the survey annually whether the local governments had appropriate information to evaluate the quality of lung cancer screening systems. On the basis of "The Lung Cancer Screening Manual" developed by the Ministry of Health, Labor and Welfare, Japan, 45 items were selected as indicators for the survey, which were the indispensable for evaluating the quality of the screening. The items could be obtained easily when the screening had been conducted according to the standard screening method. The survey was authorized by Miyagi PCMCSS in March 2001, and the questionnaire was sent to all local governments in June 2001 (Table 1). When the local government did not have the data, they would inquire to the screening provider which was commissioned the lung cancer screening from the local government. In the questionnaire, we notified them that the survey would be conducted annually, and that the results of the survey would be informed to the residents.

After several demand for submission to the municipalities which had not submitted, the questionnaires were finally collected from all municipalities until January 2002. According to the reply to the questionnaire, LCSD rated each municipality using a 5-rank classification: A: all of the items were obtained sufficiently; B: 1–4 items were insufficient; C: 5–8 items were insufficient; D: 9 or more items were insufficient; E: no reply to the survey. The survey was conducted annually since then.

In order to evaluate whether the results in this survey really influenced the quality of lung cancer screening, the municipalities were classified into two groups: Group X (municipalities which had A rank in 2001–2002 survey) and Group Y (municipalities which had B, C, or D rank in 2001–2002 survey). In 2004–2005 survey, all 58 municipalities of Group X also got A rank. On the other hand, 10 of 12 municipalities of Group Y got A rank, and remaining two got B rank. Then, average values of following three indicators were compared between the two groups: (1) the detection rate of lung cancer in all screenees; (2) the ratio of cases who actually underwent further examination to test-positive cases; (3) the ratio of number of clinical stage I lung cancer patients to number of all lung cancer patients.

Mann–Whitney *U* test, Fisher's exact test, and Student's *t*-test were used for statistical analysis. $p < 0.05$ was regarded as statistically significant.

Table 1
The questionnaire of the survey

1 The information about screenees
- 1.1 The table of the number of screenees according to gender and age (5-year stratum)
- 1.2 The number of screenees who was screened in the previous year
- 1.3 The test-positive rate
  - 1.3.1 in chest x-ray
  - 1.3.2 in sputum cytology
  - 1.3.3 in both tests
- 1.4 The case who underwent further examination/The test-positive cases
  - 1.4.1 in chest x-ray
  - 1.4.2 in sputum cytology
  - 1.4.3 in both tests

2 The information about lung cancer patient
- 2.1 The table of the number of lung cancer patients according to gender and age (5-year stratum)
- 2.2 The detection rate of lung cancer
  - 2.2.1 in all screenees
  - 2.2.2 in the screenees who was screened in the previous year
  - 2.2.3 in the screenees who was not screened in the previous year
- 2.3 The standardized detection ratio (the calculation method was in The Lung Cancer Screening Manual)
- 2.4 The detection rate of lung cancer by chest X-ray
  - 2.4.1 in all screenees
  - 2.4.2 in the screenees who was screened in the previous year
  - 2.4.3 in the screenees who was not screened in the previous year
- 2.5 The detection rate of lung cancer by sputum cytology
- 2.6 The detection rate of lung cancer only by sputum cytology (negative result by chest X-ray screening)
- 2.7 The number of clinical stage I lung cancer patients/the number of all lung cancer patients
- 2.8 Positive predictive value
  - 2.8.1 in all screenees
  - 2.8.2 in the screenees who was screened in the previous year
  - 2.8.3 in the screenees who was not screened in the previous year

3 The information of the screening system
- 3.1 Indirect chest X-ray or direct chest X-ray?
- 3.2 Maximum voltage of chest X-ray equipment
- 3.3 Exposure voltage of chest X-ray
- 3.4 Is fluorescent screen used?
- 3.5 Is magnifying paper used?
- 3.6 Is ortho-type film used?
- 3.7 The number of pulmonologist or radiologist/the number of all doctors who performed interpretation
- 3.8 Is double check in interpretation performed as described in The Lung Cancer Screening Manual?
- 3.9 Does compare with previous films of the patients as described in The Lung Cancer Screening Manual?
- 3.10 Does the conference about chest X-ray screening have?
- 3.11 Is the quality of chest X-ray films evaluated?
- 3.12 The number of radiological technicians who work at lung cancer screening
- 3.13 The number of exposures per technician per day
- 3.14 Do the technicians have opportunity to study?
- 3.15 The number of doctors who certified for cytological diagnosis
- 3.16 The number of doctors who mainly diagnose respiratory cytological specimens
- 3.17 The number of cytoscreeners
- 3.18 The number of specimens per cytoscreener per day
- 3.19 Do the cytoscreeners have opportunity to study?
- 3.20 Is double check performed in cytological screening?
- 3.21 Direct smear method or cell collection method?
- 3.22 Are the cytological findings in previous specimens of newly diagnosed patients re-evaluated?
- 3.23 Is the report of the results of further examination collected from the hospitals?

3. Results

In 2002, a total of 70 municipalities were rated, and 58, 3, 6, 3, and 0 municipalities were categorized as A, B, C, D, and E, respectively. All of the rating, with the name of municipality, was proclaimed in the website of Miyagi Prefectural Government [10].

Table 2 shows the rating of the survey in 2001–2002 according to the population of the municipality. The population of the municipalities had no association with the rank they got ($p = 0.143$, Mann–Whitney *U* test).

Each local government commissioned the lung cancer screening to one of several screening providers. Table 3 shows the rating of the survey in 2001–2002 according to the screening providers commissioned. Screening provider P and Q got more A-rank than others ($p < 0.001$, Fisher's exact test).

Table 2
The rating of the survey in 2001–2002 according to the population of the municipality

Population	Rating					Total
	A	B	C	D	E	
1–5,000	6(100%)					6
5,001–10,000	21(91%)		1	1		23
10,001–15,000	11(73%)	1	3			15
15,001–20,000	5(83%)		1			6
20,001–30,000	5(83%)			1		6
30,001–60,000	6(86%)			1		7
60,001–	5(71%)	1	1			7

Table 3
The rating of the survey in 2001–2002 according to the company commissioned

Company	Rating					Total
	A	B	C	D	E	
P	55	2				57
Q	4					4
R			3	1		4
S			2			2
T				2		2
U			1			1

Table 4
The changes of the number of insufficient items and the rank of 15 municipalities in the first 2 years (remaining 55 municipalities had A-rank in both years)

Municipality	Survey in 2001–2002		Survey in 2002–2003		Number of items improved	Number of rank improved
	Number of insufficient items	Rank	Number of insufficient items	Rank		
a	19	D	2	B	17	2
b	11	D	5	C	6	1
c	9	D	0	A	9	3
d	8	C	2	B	6	1
e	8	C	0	A	8	2
f	8	C	1	B	7	1
g	7	C	3	B	4	1
h	7	C	0	A	7	2
i	6	C	9	D	−3	−1
j	2	B	6	C	−4	−1
k	1	B	0	A	1	1
l	1	B	0	A	1	1
m	0	A	1	B	−1	−1
n	0	A	1	B	−1	−1
o	0	A	1	B	−1	−1
Total	87		31		56	10

In 2002–2003, the number of municipalities with each rating changed to 60, 7, 2, 1, and 0, which indicated that 56 more items were newly obtained in the whole prefecture (Table 4). **The results improved year by year. In 2004–2005, the number of municipalities changed to 68, 2, 0, 0, and 0** (Table 5).

Table 6 **shows the results of the changes of the average values concerning quality control in the two groups of municipalities. Although "The detection rate of lung cancer in all screenees" and "The ratio of cases who actually underwent further examination to test-positive cases" of Group Y in 2001–2002 were significantly worse than those of Group X (Student's *t*-test, $p = 0.049$ and 0.036, respectively), those differences disappeared in 2004–2005.**

Table 5
The number of the rank which local municipalities obtained in the 4 years

Year	Rank				
	A	B	C	D	E
2001–2002	58	3	6	3	0
2002–2003	60	7	2	1	0
2003–2004	65	5	0	0	0
2004–2005	68	2	0	0	0

4. Discussion

In February 2000, LCSD in Miyagi PCMCSS decided to start a new survey about quality control of the lung cancer screening. At the beginning, LCSD had to decide what kind of survey they should do, because there was a manual for screening method, but there was not a manual for quality control of screening system in Japan.

When developing the survey, following points were considered. First, the survey should be simple and could be conducted with low cost, because PCMCSS did not have enough budget or personnel. Second, the results of the survey should be concisely informed to the public, showing the comparison to other municipalities, because the residents should know the quality of the screening system in their municipalities to seek better screening system of high quality with reasonable cost. Third, the survey was to evaluate whether the screening system in each municipality achieved at least the minimally required level. Therefore, LCSD of Miyagi PCMCSS decided to conduct the annual survey with questionnaires, whether the local government had enough information to evaluate the quality of their lung cancer screening systems. The questionnaire was prudently made according to "The Lung Cancer Screening Manual", and the survey was authorized by Miyagi PCMCSS in

Table 6
The changes of the average values concerning quality control in the two groups of municipalities

	2001–2002	p value	2004–2005	p value
(1) The detection rate of lung cancer in all screenees (per 1000)				
Group				
X	0.703 (n = 58)	0.049	0.535 (n = 58)	0.979
Y	0.351 (n = 10, 2 unknown)		0.538 (n = 12)	
(2) The ratio of cases who actually underwent further examination to test-positive cases				
Group				
X	0.908 (n = 58)	0.036	0.874 (n = 58)	0.739
Y	0.838 (n = 10, 2 unknown)		0.865 (n = 12)	
(3) The ratio of number of clinical stage I lung cancer patients to number of all lung cancer patients				
Group				
X	0.512 (n = 58)	0.071	0.530 (n = 58)	0.563
Y	0.111 (n = 3, 9 unknown)		0.609 (n = 11, 1 unknown)	

March 2001. In order to avoid misunderstanding, the questionnaire required numerical value rather than Yes–No question, and we could ask to municipalities if the value was strange.

The first survey actually began in June 2001 and finished in January 2002. The result of the survey was satisfactory. Although some municipalities did not submit annual reports of lung cancer screening to LCSD until 2000 despite of several demand to submit, all of the municipalities replied the questionnaire of the survey to LCSD by January 2002. The size of the municipalities did not have an association with the rating, whereas the screening provider commissioned had, which might indicate that the screening providers R, S and T had some problems in quality control.

The results of the survey in successive years were impressive. There were several factors which influenced the results. The most important point was that LCSD declared that the results of the survey would be informed to the residents with comparison to other municipalities. The person in charge in each municipality, especially in municipalities which could not achieve A-rank, inquired many questions to LCSD during the survey. Some people even asked LCSD to postpone the announcement of the results to the residents, which was not accepted. The governor of the local government must feel social pressure when his municipality had lower-rank. After 3 years, there was no municipality which got C, D, or E, regardless of the screening provider commissioned.

By the analysis of the relation between the results of this survey and the three indicators concerning quality of lung cancer screening, two of them were significantly worse in Group Y municipalities than in Group X in 2001–2002. However, in 2004–2005, such differences were not detected. During the years, the rating of Group Y municipalities in the survey had dramatically improved (2001–2002, B: 3; C: 6; D: 3. 2004–2005, A: 10; B:2). Although this survey using the questionnaire did not directly influence these indicators, it might affect the results indirectly.

It is possible for PCMCSS to annually conduct surveys to determine whether the local government has appropriate information to evaluate the quality of lung cancer screening systems. The survey can be developed for lung cancer screening by chest CT. Even in the present system in Japan, such surveys should be done in each prefecture, announcing that the results will be informed to the residents. However, the survey is an only first step in quality control of cancer screening, and more essential, effective, and nationwide surveys should be developed.

Conflict of interest statement

None declared.

Acknowledgements

This study was supported in part by the Grant-in-Aid for Cancer Research from the Ministry of Health, Labor and Welfare, and Grant-in-Aid for Scientific Research from the Ministry of Education, Culture, Sports, Science and Technology, Japan.

References

[1] Pedersen K, Nordanger J. Quality control of the physical and technical aspects of mammography in the Norwegian breast-screening programme. Eur Radiol 2002;12:463–70.
[2] Tiele DL. Quality assurance results from a breast screening pilot study. Australas Phys Eng Sci Med 1991;14:163–8.
[3] Morimoto T, Okazaki M, Endo T. Current status and goals of mammographic screening for breast cancer in Japan. Breast Cancer 2004;11:73–81.
[4] Mattosinho de Castro Ferraz MdaC, Dall' Agnol M, di Loreto C, Pirani WM, Utagawa ML, Pereira SMM, et al. 100% rapid rescreening for quality assurance in a quality control program in a public health cytologic laboratory. Acta Cytol 2005;49:639–43.
[5] Renshaw AA. Rescreening in cervical cytology for quality control: when bad data is worse than no data or what works, what doesn't, and why. Clin Lab Med 2003;23:695–708.
[6] Bastani R, Yabroff KR, Myers RE, Glenn B. Interventions to improve follow-up of abnormal findings in cancer screening. Cancer 2004;101:1188–200.
[7] Agurto I, Sandoval J, De La Rosa M, Guardado ME, et al. Improving cervical cancer prevention in a developing country. Int J Qual Health Care 2006;18:81–6.
[8] Sobue T, Suzuki T, Naruke T. The Japanese Lung Cancer Screening Research Group. A case-control study for evaluating lung cancer screening in Japan. Int J Cancer 1992;50:230–7.
[9] Sagawa M, Nakayama T, Tsukada H, Nishii K, Baba T, Kurita Y, et al. The efficacy of lung cancer screening conducted in 1990s: 4 case-control studies in Japan. Lung Cancer 2003;41:29–36.
[10] http://www.pref.miyagi.jp/kensui/.

Oncogene (2008), 1–10

www.nature.com/onc

ORIGINAL ARTICLE

Protein phosphatase Dusp26 associates with KIF3 motor and promotes N-cadherin-mediated cell–cell adhesion

N Tanuma[1,2,7], M Nomura[1,7], M Ikeda[2], I Kasugai[1], Y Tsubaki[2], K Takagaki[2], T Kawamura[3], Y Yamashita[4], I Sato[5], M Sato[6], R Katakura[4], K Kikuchi[2] and H Shima[1]

[1]Division of Cancer Chemotherapy, Miyagi Cancer Center Research Institute, Natori, Japan; [2]Division of Biochemical Oncology and Immunology, Institute for Genetic Medicine, Hokkaido University, Sapporo, Japan; [3]Laboratory for Systems Biology and Medicine, RCAST, University of Tokyo, Tokyo, Japan; [4]Division of Neurosurgery, Miyagi Cancer Center, Natori, Japan; [5]Section of Clinical Research, Miyagi Cancer Center Research Institute, Natori, Japan and [6]Division of Thoracic Surgery, Miyagi Cancer Center, Natori, Japan

Recent studies have demonstrated essential functions for KIF3, a microtubule-directed protein motor, in subcellular transport of several cancer-related proteins, including the β-catenin–cadherin(s) complex. In this study, we report identification of the protein-phosphatase Dusp26 as a novel regulator of the KIF3 motor. Here we undertake yeast two-hybrid screening and identify Kif3a, a motor subunit of the KIF3 heterotrimeric complex, as a novel Dusp26-binding protein. Co-immunoprecipitation and colocalization experiments revealed that Dusp26 associates not only with Kif3a, but also with Kap3, another subunit of the KIF3 complex. Dephosphorylation experiments *in vitro* and analysis using mutant forms of Dusp26 in intact cells strongly suggested that Dusp26 is recruited to the KIF3 motor mainly by interaction with Kif3a, and thereby dephosphorylates Kap3. Forced expression of Dusp26, but not its catalytically inactive mutant, promoted distribution of β-catenin/N-cadherin, an established KIF3 cargo, to cell–cell junction sites, resulting in increased cell–cell adhesiveness. We also showed that Dusp26 mRNA expression was downregulated in human glioblastoma samples. These results suggest previously unidentified functions of Dusp26 in intracellular transport and cell–cell adhesion. Downregulation of Dusp26 may contribute to malignant phenotypes of glioma.
Oncogene (2008) **0**, 000–000. doi:10.1038/onc.2008.431

Keywords: •; •;

Introduction

Dual-specificity protein phosphatases (DSPs) form an evolutionarily conserved subgroup of protein-tyrosine phosphatases, originally characterized by their ability to catalyse dephosphorylation of protein phospho-Ser/Thr and phospho-Tyr residues (Camps *et al.*, 2000; Alonso *et al.*, 2004; Pulido and Hooft van Huijsduijnen, 2008). Dusp26 (also referred to as LDP-4, MKP-8 and NEAP) is a recently identified DSP protein and its function remains obscure. Expression of Dusp26 mRNA appears restricted to specific tissues such as brain and retina (Wang *et al.*, 2006; Takagaki *et al.*, 2007). The only functional motif identified thus far in Dusp26 is a DSP catalytic domain: Dusp26 does not resemble DSP molecules belonging to the MKP family, which exhibit Rhodanase domains that recognize substrate mitogen-activated protein kinases (MAPKs: Erk, JNK and p38) (Camps *et al.*, 2000). To date, reports regarding Dusp26 function have been limited to its function in the MAPK pathway. Specifically, Dusp26 has been reported to function as a p38-specific phosphatase (Vasudevan *et al.*, 2005; Yu *et al.*, 2007) and an Erk-phosphatase (Hu and Mivechi, 2006). In contrast, Wang *et al.* (2006) suggested that Dusp26 is not an MAPK phosphatase but rather negatively regulates the PI3K–Akt pathway by an unknown mechanism. In addition, Takagaki *et al.* (2007) reported that Dusp26 can potentiate JNK and p38 activation rather than inactivate it in a certain cellular contexts. Thus, the regulatory functions of Dusp26 on MAPK function are controversial. On the basis of these findings, we hypothesized that Dusp26 might interact with unidentified cofactor(s) and/or substrate(s), in addition to proteins in the MAPK cascade.

The KIF3 complex, a microtubule plus-end-directed motor and member of the kinesin superfamily (KIF), functions in transport of membrane organelles and is composed of two motor subunits, Kif3a and Kif3b, and a nonmotor subunit Kap3 (Hirokawa, 2000b). Mice lacking either Kap3 or Kif3a show loss of left–right asymmetry and embryonic lethality due to the proteins' indispensable function in formation of primary cilia and nodal flow during embryogenesis (Takeda *et al.*, 1999; Hirokawa, 2000a; Hirokawa *et al.*, 2006). The KIF3 motor is also implicated in tumorigenesis: cancer-related proteins such as APC, β-catenin–cadherin(s) and the Par3 polarity complex have been identified as KIF3-

Correspondence: H Shima, Division of Cancer Chemotherapy, Miyagi Cancer Center Research Institute, 47-1 Nodayama, Medeshima-Shiode, Natori 981-1293, Japan.
E-mail: shima-hi632@pref.miyagi.jp
[7]They contributed equally to this work.
Received 11 August 2008; revised 17 October 2008; accepted 3 November 2008

cargos (Jimbo *et al.*, 2002; Nishimura *et al.*, 2004). β-Catenin and cadherin associate with the KIF3 motor probably through interaction of β-catenin with Kap3 (Jimbo *et al.*, 2002). Conditional Kap3 knockout mice develop neuroepitherial tumors likely due to defects in post-Golgi transport of the β-catenin/N-cadherin complex to the cell periphery, resulting in abnormal β-catenin accumulation in the cytosol and nucleus (Teng *et al.*, 2005). More recently, an important function for KIF3 in regulating β-catenin-dependent gene expression in response to Wnt signaling by cilia-dependent mechanism has been reported (Corbit *et al.*, 2008).

β-Catenin/cadherin(s) subcellular localization is critical for tumorigenesis. Cadherin(s) at the plasma membrane functions in calcium-dependent cell–cell interactions whereas β-catenin links cell adhesion to activities of the actin cytoskeleton. Recent studies reveal that modulation of cell–cell contact affects cell motility and has consequences for cancer metastasis. Furthermore, defects in transport of β-catenin/cadherin(s) to the cell periphery result in aberrant accumulation of β-catenin in the cytosol as well as in the nucleus, where it together with T-cell factor (TCF) functions as a transcriptional mediator of canonical Wnt signaling. Thus proper localization of the β-catenin–cadherin complex at cell–cell junctions is essential for tumor suppression.

Here, using yeast two-hybrid screening, we identified Kif3a, a subunit of the KIF3 microtubule-dependent protein motor, as a Dusp26-interacting protein (Figure 1). We also demonstrate that Dusp26 dephosphorylates the Kap3 subunit of the KIF3 motor and enhances N-cadherin-mediated cell–cell interactions. Finally we analyse tumor samples and show that Dusp26 expression is downregulated in gliomas, suggesting it may have a tumor-suppressive function in brain tumors.

Results

Dusp26 interacts with the KIF3 kinesin motor

To search for factors interacting with Dusp26 we undertook yeast two-hybrid screening of a human embryonic brain cDNA library. One of the clones obtained encoded the Kif3a C terminus (Figure 1a). We did not detect interaction between Kif3a and Dusp25, another DSP molecule showing 24% amino-acid sequence homology with Dusp26 (Figure 1b). Physical interactions between Dusp26 and Kif3a were further confirmed by co-immunoprecipitation in cells transfected with Myc-Kif3a with or without Flag-Dusp26

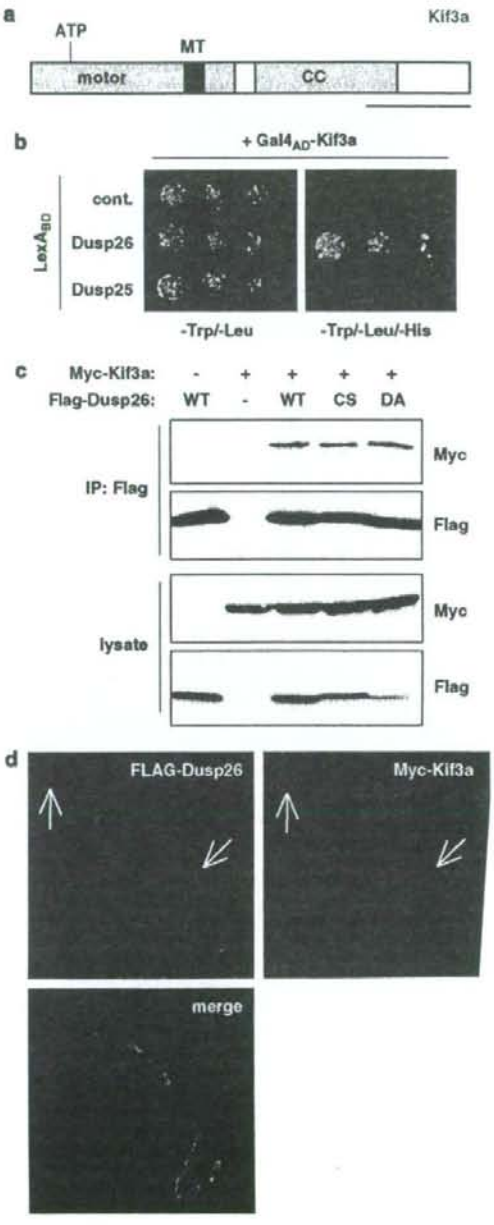

Figure 1 Dusp26 interacts with the Kif3a subunit of KIF3 motor. (**a**) Schematic structure of Kif3a. The motor domain, ATP-binding site (ATP) and microtubule-binding site (MT) therein, and coiled-coiled domain (CC) are shown. The line represents the cDNA fragment isolated in two-hybrid screening using Dusp26 as a bait. (**b**) Two-hybrid analysis showing interaction of Dusp26 with Kif3a fragment isolated in the screening. Dusp25 served as negative control. (**c**) Co-immunoprecipitation of Kif3a with Dusp26. HTO cells were transfected with Flag-tagged versions of wild-type (WT) and inactive mutant forms (CS and DA) of Dusp26, Myc-Kif3a and empty vector in combinations, immunoprecipitated with an anti-Flag antibody, and probed with anti-Myc or anti-Flag antibodies. (**d**) Kif3a and Dusp26 colocalization. HTO cells transfected with Flag-Dusp26 and Myc-Kif3a were immunostained using anti-Flag and anti-Myc antibodies, followed by anti-rabbit IgG-Alexa 488 and anti-mouse IgG-Cy3. Images shown are extended focus views obtained by maximum projection of confocal images along the Z axis. Arrows indicate overlaps of Flag-Dusp26 and Myc-Kif3a outside the Golgi.

(Figure 1c). Dusp26 protein exhibited conserved Asp and Cys residues, which are required for catalysis in all DSP family members. Substitution of these residues to Ala and Ser (Dusp26-DA and -CS, respectively) did not affect Dusp26 and Kif3a interaction, indicating that association with Kif3a does not require catalytic activity of Dusp26 (Figure 1c). Dusp26 showed cytoplasmic localization and enrichment in Golgi apparatus, as reported previously (Takagaki *et al.*, 2007), and strong colocalization of Dusp26 and Kif3a was observed (Figure 1d).

We next asked whether Dusp26 associates with Kap3, another subunit of the KIF3 motor complex. As shown in Figure 2a, Kap3, as well as Kif3a, was also efficiently co-immunoprecipitated with Dusp26. In a yeast two-hybrid assay, interaction between Dusp26 and Kap3 was relatively weak when compared to that of Dusp26-Kif3a (Figure 2b). Collectively, these results suggest that Dusp26 binds to the KIF3 motor complex, primarily through interaction with the Kif3a subunit.

Dephosphorylation of Kap3 by Dusp26

It has been reported that Kap3 is a phosphoprotein, and that its phosphorylation is regulated during cell cycle (Haraguchi *et al.*, 2006). To elucidate the significance of the Dusp26-KIF3 motor interaction, we asked whether Kap3 was a Dusp26 substrate. To this end, we analysed Kap3 phosphorylation using a recently developed phosphate-binding tag (Phos-tag) that captures phosphomonoester dianions bound to Ser, Thr and Tyr residues (Kinoshita *et al.*, 2006). As shown in Figure 3a, Kap3 expressed in HeLa cells was identified as two bands. The slower migrating band, which in this assay represents phosphorylated proteins, disappeared following treatment with bacterial λ-phosphatase *in vitro* (Figure 3b), and slightly increased in cells synchronized at G_2/M phase by treatment with demecolcine, a microtubule-disrupting reagent (Figure 3c). These find-

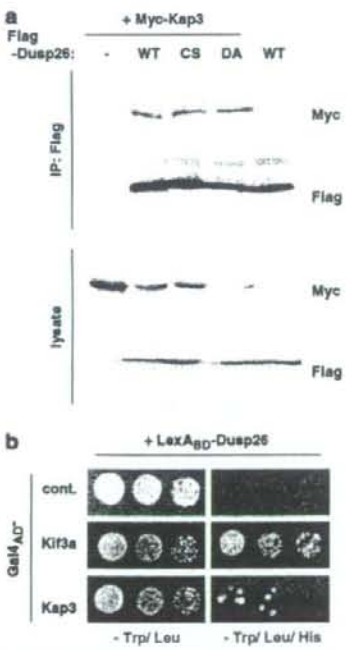

Figure 2 Interaction between Dusp26 and Kap3. (**a**) Co-immunoprecipitation of Kap3 with Dusp26. COS-7 cells were transfected with Flag-Dusp26 or its mutants together with Myc-Kap3 and analysed by co-immunoprecipitation as in Figure 1c. (**b**) Interaction between Dusp26 and Kap3 detected by two-hybrid analysis in yeast. Kif3a served as a positive control.

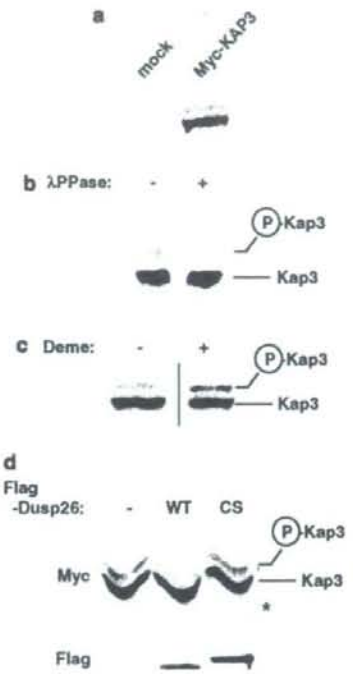

Figure 3 Negative regulation of Kap3 phosphorylation by Dusp26. (**a**) Analysis of Kap3 phosphorylation using Phos-tag/SDS–polyacrylamide gel (PAGE). Lysates from mock- or Myc-Kap3-transfected HTO cells were separated by Phos-tag/SDS–PAGE, under conditions in which phosphorylated proteins migrate more slowly than corresponding nonphosphorylated proteins, and analysed by western blotting using an anti-Myc antibody. (**b**) Identity of slower migrating Kap3 on Phos-tag/SDS–PAGE as phosphorylated Kap3. HTO cells were transfected with Myc-Kap3, lysed, and immunoprecipitated with ani-Myc antibody. Immunoprecipitates were further treated with λ-phosphatase, and subjected to Phos-tag/SDS–PAGE as in A. Myc-Kap3 was detected by western blotting. (**c**) Confirmation of increased Kap3 phosphorylation in cells at G_2/M phase. Kap3 phosphorylation of HTO cells treated with demecolcine (Deme) was analysed as in A. (**d**) Dusp26, but not its inactive mutant (CS), suppresses Kap3 phosphorylation. Myc-Kap3 was introduced into HTO cells together with wild-type (WT) or a mutant form (CS) of Dusp26 and analysed using Phos-tag/SDS–PAGE. An asterisk marks cross-reacted bands.

ings are consistent with a previous report that Kap3 phosphorylation increases as cells progress toward M-phase (Haraguchi *et al.*, 2006). Strikingly, coexpression of Dusp26 markedly decreased Kap3 phosphorylation, whereas an inactive Dusp26 mutant, Dusp26-CS, had no effect on Kap3 phosphorylation levels (Figure 3d).

To characterize Dusp26-mediated dephosphorylation of Kap3, we constructed several N-terminally truncated mutants of Dusp26 (Figure 4a). Dusp26-ΔN15 and ΔN36 suppressed Kap3 phosphorylation as well as did full-length Dusp26. By contrast, expression of Dusp26-ΔN58 did not decrease Kap3 phosphorylation (Figure 4b), indicating that the Dusp26 N terminus is essential for mediating Kap3 dephosphorylation. Notably, this region is also required for co-immunoprecipitation of Kif3a and Kap3 with Dusp26. As shown in Figure 4c, deletion of the N terminus by 36 or 58 but not 15 amino acids produced gradual decreases in Dusp26/Kif3a and Dusp26/Kap3 co-immunoprecipitations, suggesting that the entire Dusp26 N terminus contributes to the Dusp26/KIF3 interaction. Although the Dusp26 N terminus is required for Kap3 dephosphorylation and Dusp26/KIF3 association together with Figure 3b, we could not exclude the possible structural functions of this region (see below). The interaction between Dusp26 and KIF3 motor at endogenous levels was confirmed by co-immunoprecipitation of Kif3a with Dusp26 from lysate of IMR-32 neuroblastoma cells (Figure 4d). In addition, we also observed co-immunoprecipitation of N-cadherin and β-catenin with Dusp26 (see below). To determine whether Dusp26 dephosphorylates Kap3 directly, we prepared recombinant Dusp26 proteins but found that GST-Dusp26 (full length) expressed in *Escherichia coli* and His-Dusp26 translated *in vitro* using wheat germ extracts were highly insoluble, preventing analysis using these proteins. Thus we performed *in vitro* experiments using recombinant Dusp26-ΔN15 protein. Purified GST-Dusp26-ΔN15 showed vanadate-sensitive catalytic activities against a pNPP substrate in agreement with general features of PTP and DSP enzymes (Figure 4e). Incubation of cell lysate containing Kap3 with GST-Dusp26-ΔN15 *in vitro* under dephosphorylation conditions, that is, in the absence of phosphatase inhibitors, resulted in loss of phosphorylated Kap3 in a vanadate-sensitive manner (Figure 4f). In addition, purified Kap3 was also dephosphorylated by GST-Dusp26-ΔN15 *in vitro*, indicating that Kap3 is a Dusp26 substrate (Figure 4g).

In the course of this study, we found that Dusp26 can be translated from an alternative start site. Dusp26 mRNA including its 5′-untranslated region appeared to be translated mainly from a second or third in-fame ATG codon (Met11 or Met14) (Tanuma *et al.*, unpublished observations). Thus we excluded full-length Dusp26 from further analysis. Note that Dusp26-ΔN15 showed characteristics similar to full-length protein in terms of association with KIF3 and Kap3 dephosphorylation as described previously but slightly different localization from full-length protein (that is, mild enrichment in the Golgi apparatus, as shown in Figure 6).

Dusp26 enhances N-cadherin-mediated cell–cell contacts

To analyse consequences of Dusp26-mediated Kap3 dephosphorylation, stable cell lines expressing Dusp26 (ΔN15) or its inactive mutant (ΔN15CS) were developed by retroviral infection of NIH3T3 cells (Figure 5a). Expression of endogenous Dusp26 in parent NIH3T3 cells was under the detection limit by western blot and immunohistochemical analysis (see below). After drug selection, pools of cells were analysed to avoid clonal variation. As KIF3 was implicated in intracellular transport of N-cadherin, aggregation assays were performed to examine the effect of Dusp26 on cell–cell adhesion. As shown in Figures 5b and c, NIH3T3 cells expressing Dusp26-ΔN15 (NIH3T3-ΔN15) showed more rapid aggregate formation than did cells infected with vector only (NIH3T3-vector) or with Dusp26-ΔN15CS (NIH3T3-ΔN15CS). Increased adhesiveness of NIH3T3-ΔN15 cells was lost when $Ca2^+$-dependen adhesion was blocked by EGTA, suggesting tha Dusp26 specifically enhances $Ca2^+$-dependent cel adhesion (Figure 5b). Western blotting of lysates fror stable lines indicated little change in total N-cadheri levels in these cells (Figure 5a). Immunostainin revealed that N-cadherin was localized to the cytoplasn to cell–cell contact sites, to the ruffling membrane and t tips of membrane protrusions in NIH3T3-vector ar NIH3T3-ΔN15 cells seeded at subconfluent densiti (Figure 6a). In these conditions, colocalization N-cadherin and Dusp26-ΔN15 was observed at t

Figure 4 Dusp26 dephosphorylates Kap3. (**a**) Diagram of wild-type and N-terminally truncated Dusp26 proteins. The dual-specificity protein phosphatase (DSP) catalytic domain is shown by shaded box. (**b**) The Dusp26 N-terminal region contributes to suppression of Kap3 phosphorylation. HTO cells were transfected with Flag-Dusp26 constructs depicted in A together with Myc-Kap3. Kap3 phosphorylation was analysed by Phos-tag/SDS–PAGE as in Figure 3. (**c**) Co-immunoprecipitation of KIF3 subunits with Dusp26 proteins. HTO cells were transfected with full-length or deletion mutants of Flag-Dusp26 with Myc-Kap3 and Myc-Kif3a, immunoprecipitated with an anti-Flag antibody, and immunoblotted. (**d**) Co-immunoprecipitation of KIF3 with endogenous Dusp26. IMR-32 cells were lysed and immunoprecipitated with an anti-Dusp26 antibody or control normal immunoglobulin G (IgG). Western blotting was performed using anti-Kif3a, anti-N-cadherin, anti-β-catenin and anti-Dusp26 antibodies. An asterisk marks cross-reacted and unrelated bands. (**e**) Characterization of purified recombinant Dusp26 protein. The ΔN form of Dusp26 was expressed as a GST-fusion protein in *E. coli* and purified. Left panel shows Coomassie staining of purified Dusp26-ΔN15. Asterisk marks fragment cleaved during the expression/purification process, likely composed of glutathione *S*-transferase (GST) alone. The catalytic activity of the purified enzyme was measured in the presence or absence of vanadate using substrate pNPP and shown in the right panel. (**f**) Dephosphorylation of Kap3 by Dusp26 *in vitro*. *In vitro* dephosphorylation reactions were performed as described in 'Materials and methods', and analysed for Kap3 phosphorylation by Phos-tag/SDS–PAGE followed by western blotting. Severe distortion of the bands, seen in repeated experiments, was likely due to vanadate acting as pseudo-phosphate, and thereby disturbed Phos-tag/protein interactions. (**g**) Dephosphorylation experiments were performed, as in (**f**), using immunopurified Kap3.

membrane ruffle but not at cell–cell contact sites. When cells were cultivated at higher density to allow cell–cell contacts, N-cadherin was concentrated at contact sites in NIH3T3-vector cells (Figure 6b). Strikingly, accumulation of N-cadherin at the cell periphery was much more pronounced in NIH3T3-ΔN15 cells and correlated with virtual loss of cytosolic N-cadherin, in contrast to NIH3T3-vector and NIH3T3-ΔN15CS cells. Similar results were obtained when cells were stained for β-catenin (Figure 6c). Overall, these results suggest that Dusp26 promotes N-cadherin-mediated cell–cell adhesion. We also generated cells expressing Dusp26-ΔN58 mutant. Neither cell adhesiveness nor N-cadherin/β-catenin localization was affected by the Dusp26-ΔN58 but its expression was low (Supplementary Figure 1a and data not shown). This was probably due to its misfolding of the mutant protein since recombinant GST-Dusp26-ΔN58 showed little pNPPase activity (Supplementary Figure 1b). Thus it remains not clear whether the Dusp26 N-terminal region is directly

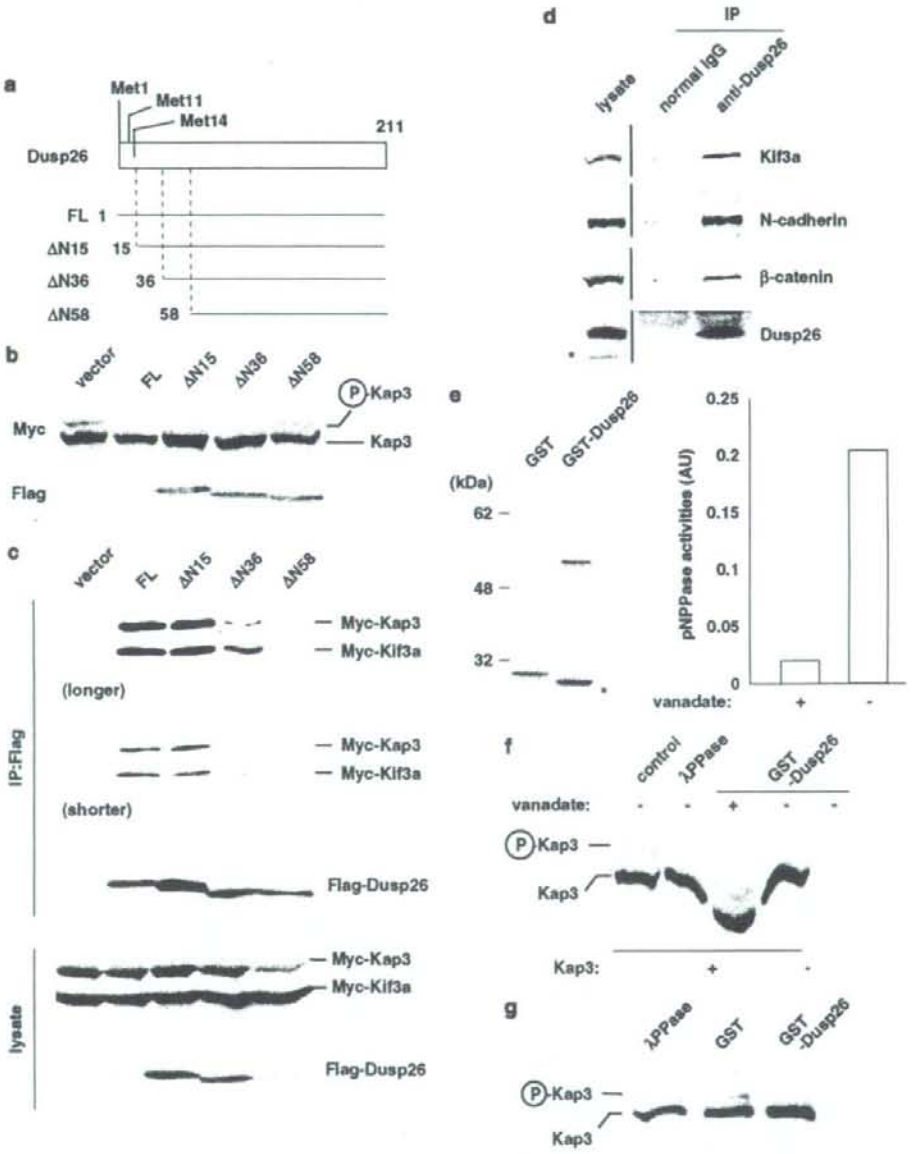

Figure 5 Enhanced cell–cell adhesion of cells expressing Dusp26. (**a**) Western analysis of NIH3T3 cells infected with retroviral vector encoding Dusp26 (ΔN15 form and its inactive mutant; see text for details) or the empty vector. After drug selection, cells were seeded on collagen-coated dishes and immunoblotted with antibodies shown at the left. (**b**, **c**) Enhanced adhesiveness of NIH3T3 cells expressing Dusp26. Aggregation assays were performed as described in 'Materials and methods'. Some representative photographs of assays are shown in (**b**). The extent of cell aggregation was calculated by the aggregation index $(N_0-N_{20})/N_0$, where N_{20} is the total particle number after a 20 min incubation and N_0 is the total particle number at the initiation of incubation, and is shown in (**c**). Data represented are averages of three independent assays with s.d. ($^*P<0.05$).

involved in association with Kif3a/Kap3 while it is required for mediating both Kap3 dephosphorylation and increased cell adhesiveness.

Downregulation of Dusp26 expression in human brain tumors

Previous studies revealed preferential Dusp26 expression in brain and that Dusp26 mRNA is broadly expressed in neuronal and glial populations throughout the brain, except in hippocampus (Takagaki *et al.*, 2007). We undertook qRT-PCR analysis of human glioblastoma samples and found that Dusp26 mRNA was downregulated in eight of nine patients evaluated (Figure 7a). Together with findings that cell–cell adhesion is enhanced in cells expressing Dusp26, these results suggest tumor-suppressing activities of Dusp26 and raise the possibility that the extent of Dusp26 downregulation correlates with invasive phenotypes of glioblastomas.

Discussion

Cadherin-mediated cell–cell adhesion plays pivotal functions for regulation of cell proliferation, differentia-

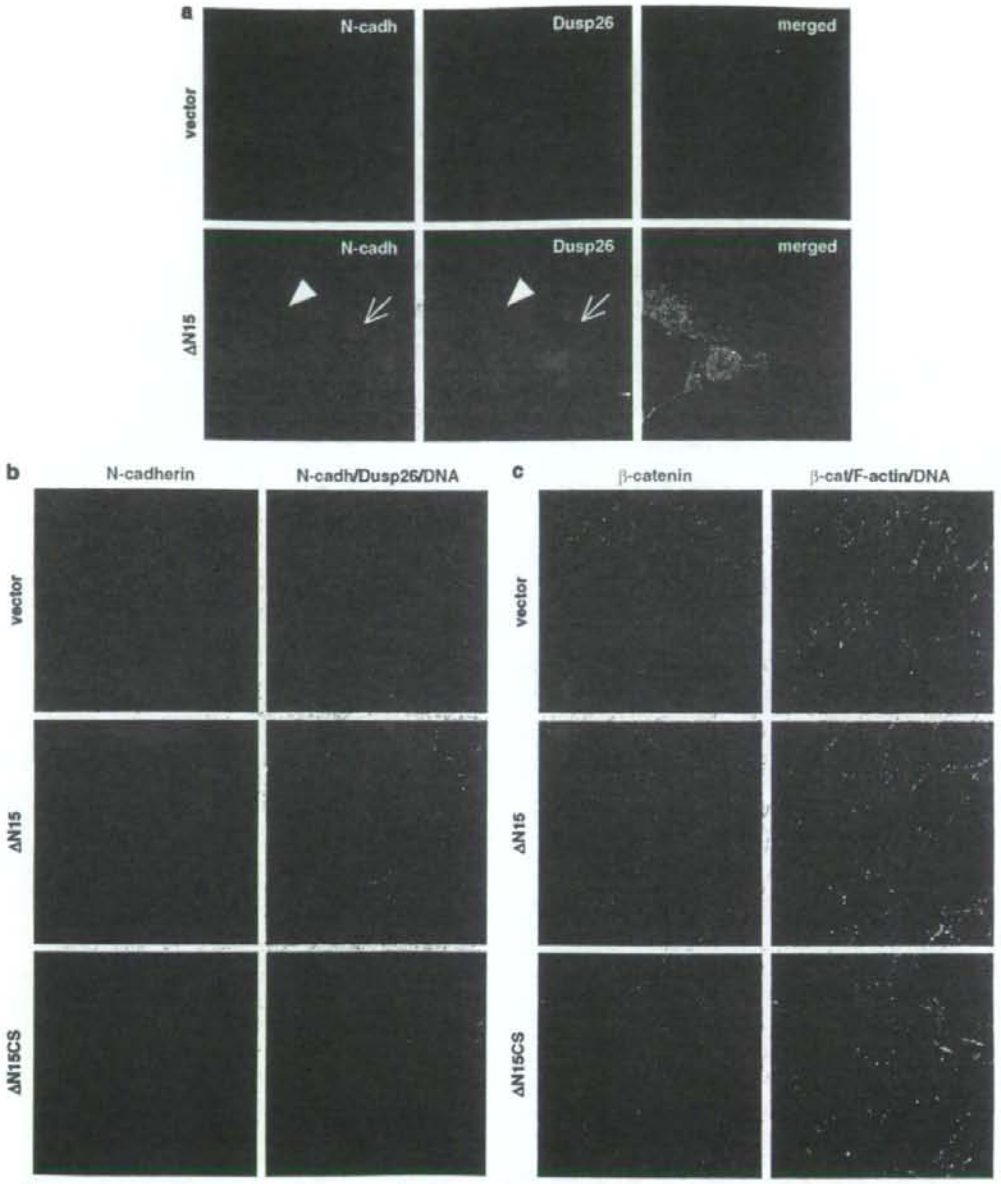

Figure 6 Enhanced N-cadherin and β-catenin localization at cell–cell contact sites of cells expressing Dusp26. (**a**) Representative images of immunostaining of NIH3T3 cells infected with Dusp26 or vector alone. Cells on coverslips coated with collagen and seeded at low density were immunostained with anti-N-cadherin (N-cadh) and anti-Dusp26 (Dusp26) antibodies. Shown are single sections obtained by confocal scans. Note Dusp26 and N-cadherin colocalization at the membrane ruffle (indicated by arrows) but not at cell–cell contact sites (arrowhead), where N-cadherin is also enriched. (**b**, **c**) Enhanced N-cadherin (**b**) and β-catenin (**c**) localization at cell–cell contact sites mediated by Dusp26. Cells were seeded at higher densities to allow contact and analysed for N-cadherin (N-cadh) and Dusp26 (**b**), and for β-catenin (β-cat) and F-actin (**c**). DRAQ5 staining shows similar cell densities of the fields.

tion and polarity, and overall has significant effect on tissue architecture. Altered adhesiveness is often associated with increased cell motility, invasiveness and tumor metastasis. We have shown that Dusp26 dephosphorylates the Kap3 subunit of the KIF3 motor and promotes localization of N-cadherin/β-catenin to sites

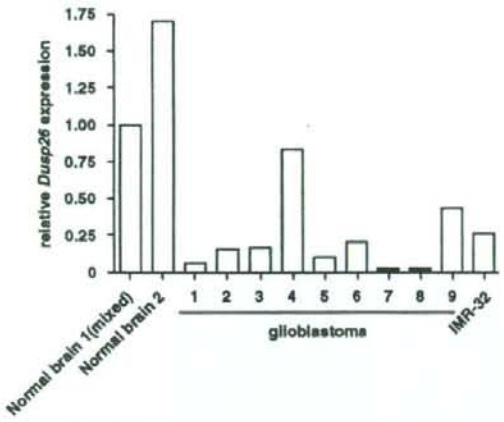

Figure 7 Analysis of Dusp26 mRNA levels in primary tumor samples. Downregulation of Dusp26 mRNA in primary glioblastoma samples and a neuroblastoma cell line. Expression levels of Dusp26 mRNA in human primary glioblastoma samples were estimated by qRT-PCR. Results were normalized to mRNA levels of the housekeeping gene porphobilinogen deaminase (*PBGD*) and shown as relative to mRNA levels seen in normal brain (normal brains (mixed)), which was set as 1.0. Also shown is Dusp26 expression in the human IMR-32 neuroblastoma cell line.

of cell–cell contact, resulting in enhanced adhesion. It has been established that post-Golgi transport of β-catenin/Cadherin(s) to the plasma membrane is mediated by the KIF3 motor (Jimbo *et al.*, 2002; Teng *et al.*, 2005). Although the detailed mechanisms by which Dusp26 enhances distribution of N-cadherin/β-catenin remain unclear, they likely involve Kap3 dephosphorylation by Dusp26, since expression of its inactive mutant does not alter Ca^{2+}-dependent adhesion (Figure 5) or N-cadherin localization (data not shown). Accumulated evidence reveals the importance of molecular motors such as myosin, dynein and KIF proteins in organelle transport, but it remains largely unknown how binding and release of cargo at destination sites are regulated. Our results suggest a possible function for Kap3 phosphorylation in these processes. Previous studies in which phosphorylation of the myosin-V and KIF17 motors by calcium/calmodulin-dependent protein kinase II were suggested to control docking of cargo (Karcher *et al.*, 2001; Guillaud *et al.*, 2008) support our hypothesis. Identification of Kap3 phosphorylation site(s) is the next critical step to address these issues.

Analysis of human glioblastoma revealed that *Dusp26* expression was low compared to that seen in normal brain in most samples. Given that cell–cell adhesion was enhanced in cells expressing Dusp26, these results suggest tumor-suppressing activities of Dusp26, and that *Dusp26* gene is silenced and/or deactivated in glioma. Dusp26 downregulation may be associated with invasive phenotypes of glioblastomas, although mechanisms underlying Dusp26 downregulation are not known.

In summary, Dusp26 dephosphorylates Kap3, enhances cell–cell adhesion by promoting localization of N-cadherin/β-catenin at sites of cell–cell contact and is downregulated in human glioblastomas. Further investigation to elucidate mechanisms regulating Dusp26 expression in brain tumors and identify kinase(s) responsible for Kap3 phosphorylation is required to understand how dysregulation of intracellular transport and cell–cell adhesion coincides with tumor development.

Materials and methods

Antibodies

Anti-Flag M2 and anti-Myc 9E10 antibody were purchased from Sigma (MO, USA) and Roche (Basel, Switzerland), respectively. Anti-β-Catenin, anti-N-Cadherin, anti-Kap3 and anti-Kif3a monoclonal antibodies were from BD Transduction (San Jose, CA, USA). Polyclonal anti-Dusp26 antibodies were described previously (Takagaki *et al.*, 2007).

Yeast two-hybrid screening

Full-length cDNA encoding human Dusp26 was subcloned into pBTM116-HA and used as bait to screen a human fetal brain cDNA library subcloned into pACT II (Clontech Laboratories Inc., Mountain View, CA, USA). The L40 yeast strain was transformed with bait and library plasmids, and about 3×10^6 clones were screened. A total of 22 positive clones were obtained and sequenced.

Cell culture, transfection and retrovirus infection

HeLa-TetOff (Clontech) and COS-7 cells were transfected using Fugene6 (Roche, Mannheim, Germany) reagent following the manufacturer's recommendation. Dusp26 expression plasmids were described previously (Takagaki *et al.*, 2007). Human Kif3a and Kap3 cDNAs were subcloned into pCMV-Myc (Clontech). For stable transfection, Flag-tagged Dusp26 cDNAs were subcloned into the retroviral vector pMXs-puro. The packaging line (PLAT-E cells; Morita *et al.*, 2000) was grown in Dulbecco's modified Eagle's medium (DMEM) with 10% fetal calf serum (FCS) and transfected with a series of pMXs-puro-Dusp26 plasmids using Fugene 6. The medium was changed the next day and further cultured for 1 day. Supernatants were used to infect NIH3T3 cells in the presence of polybrene at 7.5 μg/ml for 5 h. Infectants were selected and maintained in medium plus puromycin. Human ATC cell lines 8305C, 8505C and HTC/C3 were obtained from the Health Science Research Resources Bank (Ibaraki, Japan). 8505C and HTC/C3 cells were cultured in DMEM with 10% FCS. 8305C cells were maintained using MEM with 10% FCS. The human IMR-32 neuroblastoma line was from RIKEN and cultured in MEM supplemented with nonessential amino acids (Gibco) and 10% FCS.

Western blot analysis

Immunoprecipitation and western blotting were performed as described (Takagaki *et al.*, 2007). To analyse Kap3 phosphorylation, cells were washed in Hepes buffer twice, harvested and lysed in radioimmunoprecipitation assay buffer by sonication using Bio-ruptor (CosmoBio, Tokyo, Japan). Samples were separated on a 6% SDS–polyacrylamide gel, with 50 μM Phos-tag acrylamide (ALL-107) and 100 μM $MnCl_2$. Gels were soaked in transfer buffer with 5 mM EDTA for 10 min and electrotransferred.

Immunohistochemistry

Cells were seeded on collagen-coated coverslips in 12-well plates at 2.5×10^4 cells per well (subconfluent condition) and fixed on the next day. To obtain confluent monolayers, cells were seeded at 2×10^5 cells per well, cultured for 2 days and fixed. Immunostaining was performed as described (Takagaki *et al.*, 2007) except images were obtained using a Pascal confocal laser-scanning microscope (Zeiss). DRAQ5, a fluorescent DNA probe was obtained from Alexis (Lausen, Switzerland).

Phosphatase assay and dephosphorylation of Kap3 in vitro

GST-Dusp26-ΔN15 was expressed in the *E. coli* DH5α strain using the pGEX system (GE Healthcare UK Ltd., Buckinghamshire, UK) and purified using glutathione sepharose 4B following the manufacturer's recommendations. pNPPase assays were performed as described previously (Takagaki *et al.*, 2007). For *in vitro* Kap3 dephosphorylation experiments, Kap3 was prepared by sonication of cells transfected with Myc-Kap3 in buffer (50 mM Tris-Cl, 150 mM NaCl, 10% glycerol, 0.1% Triton X-100). Cleared lysates were supplemented with dithiothreitol (DTT) at 5 mM and incubated with or without GST-Dusp26-ΔN15 at 30 °C for 3 h in the presence or absence of 1 mM vanadate. In Figure 4g, Myc-Kap3 was immunopurified from cells transfected Myc-Kap3 using anti-Myc-Agarose (Sigma).

Cell aggregation assays

Cells were trypsinized in phosphate-buffered saline supplemented with 2 mM $CaCl_2$, suspended in medium, washed with and then resuspended in medium, passed through a 27 G needle three times, and adjusted to 5×10^5 cells per ml. Cells were incubated in 1.5 ml tubes with gentle rotation at 37 °C to allow aggregate formation. After 20 min, aliquots of the suspension were evaluated and the extent of aggregation calculated by the index $(N_0-N_{20})/N_0$, where N_{20} is the total particle number after 20 min incubation and N_0 is the total particle number at the initiation of incubation, as described previously (Ozawa *et al.*, 1990). One-way analysis of variance combined with Tukey's test was used to analyse data with unequal variance between each group. A probability level of 0.05 was considered significant.

Primary tumor samples, qRT-PCR and qGenomic-PCR analysis

Human glioblastoma samples were obtained with informed consent from nine patients at the time of surgical removal at the Division of Neurosurgery, Miyagi Cancer Center. Histological diagnoses were based on WHO (World Health Organization) criteria by a neuropathologist. RNA analyses were approved by the institutional review of Miyagi Cancer Center. RNAs were prepared using Isogen (Nippon Gene, Tokyo, Japan) reagent and reverse-transcribed using oligo-dT primer and Superscript III RTase (Invitrogen). Relative amounts of Dusp26 cDNA were quantified using the LightCycler 480, a LightCycler 480 probes master kit, TaqMan probe no. 79 from the universal probe library (Roche), and the Dusp26-specific primers (sense) 5′-GCTGCCGACTT CATCCAC-3′ and (antisense) 5′-CAGCACAATGCACCAG GAT-3′. Relative amounts of porphobilinogen deaminase (PBGD) mRNA was simultaneously estimated similarly using TaqMan probe no. 25 and specific primers (sense) 5′-AGCTATGAAGGATGGGCAAC-3′ and (antisense) 5′-TTGTATGCTATCTGAGCCGTCTA-3′. Human brain (frontal lobe) total RNAs from a pool of four different donors and from single donor were obtained from Clontech and BioChain Institute (Hayward, CA, USA), respectively.

Acknowledgements

We acknowledge Dr Konomi Kamada (Hokkaido University, Japan) for kindly providing the plasmid pBTM116-HA, the L40 yeast strain and *E. coli* HB101, and Dr Toshio Kitamura (University of Tokyo, Japan) for the pMX-puro plasmid and PLAT-E cells. Thanks are also due to E Yoshida for secretarial assistance. This work was supported in part by Grants-in-Aid for Scientific Research (B) and Grants-in-Aid for Scientific Research (C) provided by the Japan Society for the Promotion of Science of Japan.

References

Alonso A, Sasin J, Bottini N, Friedberg I, Friedberg I, Osterman A *et al.* (2004). Protein tyrosine phosphatases in the human genome. *Cell* **117**: 699–711.

Camps M, Nichols A, Arkinstall S. (2000). Dual specificity phosphatases: a gene family for control of MAP kinase function. *FASEB J* **14**: 6–16.

Corbit KC, Shyer AE, Dowdle WE, Gaulden J, Singla V, Chen MH *et al.* (2008). Kif3a constrains beta-catenin-dependent Wnt signalling through dual ciliary and non-ciliary mechanisms. *Nat Cell Biol* **10**: 70–76.

Guillaud L, Wong R, Hirokawa N. (2008). Disruption of KIF17-Mint1 interaction by CaMKII-dependent phosphorylation: a molecular model of kinesin-cargo release. *Nat Cell Biol* **10**: 19–29.

Haraguchi K, Hayashi T, Jimbo T, Yamamoto T, Akiyama T. (2006). Role of the kinesin-2 family protein, KIF3, during mitosis. *J Biol Chem* **281**: 4094–4099.

Hirokawa N. (2000a). Determination of Left-Right Asymmetry: Role of Cilia and KIF3 Motor Proteins. *News Physiol Sci* **15**: 56.

Hirokawa N. (2000b). Stirring up development with the heterotrimeric kinesin KIF3. *Traffic* **1**: 29–34.

Hirokawa N, Tanaka Y, Okada Y, Takeda S. (2006). Nodal flow and the generation of left-right asymmetry. *Cell* **125**: 33–45.

Hu Y, Mivechi NF.. (2006). Association and regulation of heat shock transcription factor 4b with both extracellular signal-regulated kinase mitogen-activated protein kinase and dual-specificity tyrosine phosphatase DUSP26. *Mol Cell Biol* **26**: 3282–3294.

Jimbo T, Kawasaki Y, Koyama R, Sato R, Takada S, Haraguchi K *et al.* (2002). Identification of a link between the tumour suppressor APC and the kinesin superfamily. *Nat Cell Biol* **4**: 323–327.

Karcher RL, Roland JT, Zappacosta F, Huddleston MJ, Annan RS, Carr SA *et al.* (2001). Cell cycle regulation of myosin-V by calcium/calmodulin-dependent protein kinase II. *Science* **293**: 1317–1320.

Kinoshita E, Kinoshita-Kikuta E, Takiyama K, Koike T. (2006). Phosphate-binding tag, a new tool to visualize phosphorylated proteins. *Mol Cell Proteomics* **5**: 749–757.

Morita S, Kojima T, Kitamura T. (2000). Plat-E: an efficient and stable system for transient packaging of retroviruses. *Gene Ther* **7**: 1063–1066.

Nishimura T, Kato K, Yamaguchi T, Fukata Y, Ohno S, Kaibuchi K. (2004). Role of the PAR-3-KIF3 complex in the establishment of neuronal polarity. *Nat Cell Biol* **6**: 328–334.

Ozawa M, Ringwald M, Kemler R. (1990). Uvomorulin–catenin complex formation is regulated by a specific domain in the

cytoplasmic region of the cell adhesion molecule. *Proc Natl Acad Sci USA* **87**: 4246–4250.

Pulido R, Hooft van Huijsduijnen R. (2008). Protein tyrosine phosphatases: dual-specificity phosphatases in health and disease. *FEBS J* **275**: 848–866.

Takagaki K, Shima H, Tanuma N, Nomura M, Satoh T, Watanabe M *et al.* (2007). Characterization of a novel low-molecular-mass dual specificity phosphatase-4 (LDP-4) expressed in brain. *Mol Cell Biochem* **296**: 177–184.

Takeda S, Yonekawa Y, Tanaka Y, Okada Y, Nonaka S, Hirokawa N. (1999). Left-right asymmetry and kinesin superfamily protein KIF3A: new insights in determination of laterality and mesoderm induction by kif3A-/- mice analysis. *J Cell Biol* **145**: 825–836.

Teng J, Rai T, Tanaka Y, Takei Y, Nakata T, Hirasawa M *et al.* (2005). The KIF3 motor transports N-cadherin and organizes the developing neuroepithelium. *Nat Cell Biol* **7**: 474–482.

Vasudevan SA, Skoko J, Wang K, Burlingame SM, Patel PN, Lazo JS *et al.* (2005). MKP-8, a novel MAPK phosphatase that inhibits p38 kinase. *Biochem Biophys Res Commun* **330**: 511–518.

Wang JY, Lin CH, Yang CH, Tan TH, Chen YR. (2006). Biochemical and biological characterization of a neuroendocrine-associated phosphatase. *J Neurochem* **98**: 89–101.

Yu W, Imoto I, Inoue J, Onda M, Emi M, Inazawa J. (2007). A novel amplification target, DUSP26, promotes anaplastic thyroid cancer cell growth by inhibiting p38 MAPK activity. *Oncogene* **26**: 1178–1187.

Supplementary Information accompanies the paper on the Oncogene website (http://www.nature.com/onc)

Biochemical and Biophysical Research Communications 377 (2008) 685–688

Contents lists available at ScienceDirect

Biochemical and Biophysical Research Communications

journal homepage: www.elsevier.com/locate/ybbrc

The methylation status of *FBXW7 β-form* correlates with histological subtype in human thymoma

Zhaodi Gu [a,1], Hidetoshi Mitsui [a,1], Kenichi Inomata [a], Masako Honda [b], Chiaki Endo [b], Akira Sakurada [b], Masami Sato [c], Yoshinori Okada [b], Takashi Kondo [b], Akira Horii [a,*]

[a] Department of Molecular Pathology, Tohoku University School of Medicine, 2-1 Seiryo-machi, Aoba-ku, Sendai, Miyagi 980-8575, Japan
[b] Department of Thoracic Surgery, Institute of Development, Aging, and Cancer, Tohoku University, 4-1 Seiryo-machi, Aoba-ku, Sendai, 980-8575, Japan
[c] Division of Thoracic Surgery, Miyagi Cancer Center Hospital, 47-1 Medeshima-Shiote-aza Nodayama, Natori, 981-1293, Japan

ARTICLE INFO

Article history:
Received 7 October 2008
Available online 18 October 2008

Keywords:
Methylation
FBXW7 β-form
Thymoma

ABSTRACT

FBXW7 is reported to be a tumor suppressor gene, and the functional inactivation of FBXW7 has been reported in various human tumors. In this study, we investigated the *FBXW7* gene in human thymoma; although no mutations were evident, a significantly high frequency of methylation in the *FBXW7 β-form* promoter was observed in types B1 or higher ($P = 0.014$). We propose a novel mechanism for the pathogenesis of thymoma by *FBXW7 β-form* and hypothesize that expressional suppression plays an important role in the malignant potential of thymoma.

Although the incidence of thymoma is 1–5/million population/year [1], it is the most frequently observed thymic epithelial tumor and the most commonly observed mediastinal tumor. This tumor frequently associates with myasthenia gravis and other paraneoplastic syndromes such as hypogammaglobulinemia, pure red cell aplasia, Graves disease, or Cushing syndrome; all of these deteriorate the quality of life (QOL) of the patients. A histological classification system for thymoma was previously proposed by Masaoka et al. [2], changed by WHO in 1999 [3], and revised in 2004 [1]. Thymoma is now classified into several histological subtypes: five major types (type A, AB, B1, B2, and B3) and others. Several studies have sought significant correlations among clinical and pathological results [4–7]; these reports suggest that type A thymoma is the most favorable; then the prognoses gradually deteriorate from type B2 to type B3.

FBXW7 (F-box and WD40 domain protein 7) is one of the ubiquitin ligases that catalyzes promoting proteins for cell proliferation, such as CCNE1, MYC, AURKA, NOTCH1, and JUN [8]. Mutations of this gene are reported in a variety of human tumors such as endometrial, pancreatic and colorectal cancers and leukemia [9–15], and FBXW7 has been suggested to function as a tumor suppressor. We determined that *FBXW7 β-form* was suppressed and highly methylated in normal peripheral blood cells [16]. Furthermore, abnormalities of *FBXW7* have been reported in T cell-originated lymphomas and leukemias [15,17,18]. Hence, it is of great interest to analyze *FBXW7* in human thymoma, one of the major tumors of the important T cell-associated organs. In the present study, we report our findings that the methylation status of *FBXW7 β-form* correlates with a high malignant potential in human thymoma.

Materials and methods

Tumors analyzed in this study. A total of 13 specimens of human thymoma, surgically resected in Tohoku University Hospital (Sendai, Japan) between July 2004 and October 2006, were analyzed in this study. Tumor cells were collected under the microscope [19]; tumor cellularity was quite high in all the tumor specimens in this study. The list of patients is summarized in Table 1. According to the WHO classification [1], these 13 tumors were classified as follows: 1 type A, 3 type AB, 5 type B1, 3 type B2, and 1 type B3. The specimens were collected under written informed consent, and the study was approved by the Ethics Committee of Tohoku University School of Medicine.

DNA extraction and mutation search. Genomic DNAs were extracted using Nucleon™ BACC2 Genomic DNA Extraction Kit for Blood & Cell Cultures (Amersham Biosciences, Little Chalfont, UK) following the manufacturer's protocol. The purified DNAs were PCR amplified for the whole exons and their intron–exon boundaries of *FBXW7* by methods described previously [19] with the GeneAmp PCR system 9700 (Applied Biosystems, Foster City, CA). Primer pairs for individual exons and PCR conditions are described previously [20], and the nucleotide sequences were determined by methods described previously [21] using the Hi Di Formamide (Applied Biosystems) and ABI PRISM3100 Genetic Analyzer (Applied Biosystems).

* Corresponding author. Fax: +81 22 717 8047.
E-mail address: horii@m.tains.tohoku.ac.jp (A. Horii).
[1] These authors contributed equally to this work.

0006-291X/$ - see front matter © 2008 Elsevier Inc. All rights reserved.
doi:10.1016/j.bbrc.2008.10.047

Table 1
Tumors analyzed in this study.

Case	Age	Sex	Type	Methylation status
1	66	F	B1	M
2	56	F	B3	P
3	82	F	A	U
4	35	F	B2	P
5	69	F	B1	M
6	73	F	AB	U
7	66	M	B2	P
8	61	M	B2	M
9	74	M	AB	U
10	68	M	AB	P
11	67	F	B1	M
12	43	F	B1	M
13	77	F	B1	M

Genomic sodium bisulfite sequencing analysis. Genomic sodium bisulfite sequencing analysis was performed by methods described previously [22] using each 1 μg of genomic DNA and CpGenome™ DNA Modification Kit (Chemicon, Temecula, CA). The modified DNA was used as a template for PCR amplifications with primers 5′-TAAAATGTTTTTGAAAAGATTTATTTG-3′ and 5′-TATTTTTCCCCTTCAATAATTCTATA-3′ [16], and the nucleotide sequences of the amplified products were determined by a method described previously [21].

Statistics. Statistical calculation was done using Statview software (SAS Institute Inc., Cary, NC).

Results and discussion

Mutation analyses

In this study, we analyzed mutations in 13 resected thymoma specimens. The entire exonic region (exons α, β, and γ, corresponding to the first exon for each of the α-, β-, and γ-form of the transcript, and the common exons 2 through 11) of the *FBXW7* gene was surveyed by sequencing the genomic DNAs. No mutations were detected.

Determination of the methylation status in the promoter region of FBXW7 β-form

We previously demonstrated that the expression of the *FBXW7* β-form is specifically suppressed in human glioma cell lines as well as peripheral blood cells [16,20]. Furthermore, the promoter and the 5′ region in exon 1 of *FBXW7 β-form* are specifically methylated in peripheral blood cells [16]. Because abnormalities of *FBXW7* have been reported in T cell lymphomas and leukemias [15,17,18], we determined the methylation status in our series of thymoma specimens by the sodium bisulfite-modification method followed by sequencing analysis. The analyzed region is illustrated in Fig. 1A, and representative results of the sequencing analyses are shown in Fig. 1B. According to the sequencing results, we classified the methylation status for each CpG site into one of three groups; highly methylated (+), partially methylated (+/−), and unmethylated (−).

Table 2
Summary of methylation status.

Type	M or P	U
A or AB	1	3
B1–B3	9	0

$P = 0.014$ by Fisher's exact test.

The methylation status for each of the 13 tumors is summarized in Table 1 and schematically illustrated in Fig. 1C. Results clearly indicated the methylation status for individual tumors. We designated the three categories as methylated (M), partially methylated (P), and unmethylated (U). Based on this classification, patient #6 (type AB) is unmethylated (U), #11 (type B1) is methylated (M), and #7 (type B2) is partially methylated (P). Unfortunately, no mRNA samples were available, so we could not further analyze the expression levels of *FBXW7 β-form* in these tumors.

Methylation status significantly correlates with histological classification

We analyzed our present results to see if there is any association between methylation status and histological subtypes, and a significant correlation was observed. When we divided our samples into two groups (types A and AB, and types B1 through B3), a positive association between methylation status and histological classification was observed, as shown in Table 2 ($P = 0.014$ by Fisher's exact test). Our present results suggest that the *FBXW7 β-form* plays an important role in the development and progression of thymoma and that inactivation of this gene is one of the crucial factors in changing the tumors into those with higher malignant potential.

Conclusion

In the present study, we found for the first time that methylation status positively correlates with histological classification of human thymoma. This novel finding will contribute to not only better understanding of the molecular pathogeneses of thymoma, but also to accurate diagnosis of the disease. Furthermore, may also be possible to open up novel therapeutic approaches it for thymoma utilizing this cell cycle negative regulator protein.

Acknowledgments

We are grateful to Dr. Barbara Lee Smith Pierce (University of Maryland University College) for editorial work in the preparation of this manuscript. This work was supported in part by Grants-in-Aid, the 21st Century COE Program Special Research Grant, and Academic Frontier Project for Private Universities: matching fund subsidy 2006–2010 from the Ministry of Education, Culture, Sports, Science and Technology of Japan, and by a Grant-in-Aid for Cancer Research from the Ministry of Health, Labour and Welfare of Japan.

Fig. 1. (A) Nucleotide sequences of the putative promoter and 5′ region of exon 1 of *FBXW7 β-form* are shown, and the CpG sites are underlined. Arrows indicate the positions of primers used in the sodium bisulfite sequence assay. Binding sites for transcription factors along with the translational initiation codon (ATG) are boxed with thin lines, and the nucleotide sequences shown in (B) are boxed with thick lines. Nucleotide numbers were corrected because the database has been updated since our previous report [16]. (B) Representative results of the genomic sequencing analyses of the *FBXW7 β-form* after sodium bisulfite-modification. The black dot indicates the cytosine residues in CpG sequences with complete methylation; high peaks for C are observed. Gray dots indicate partial methylation; double peaks for C and T are observed. White dots indicate no methylation; only a single peak for T is observed. Cytosine residues that were converted to thymine after modification at the non-CpG sites are indicated by triangles. (C) The methylation status for each individual tumor is schematically illustrated. Vertical bars on top indicate the relative location of the CpG sites. The CAP site and translational initiating codon (ATG) are also indicated. Black and white dots represent methylated and unmethylated CpG sites, respectively, and the gray dots indicate partially methylated CpG sites. The nucleotide sequences shown in (B) are boxed. M, methylated; P, partially methylated; U, unmethylated.